Department of Precision and Microsystems Engineering

Dynamical Mechanical Metamaterials for Path Generation

Tom Vreugdenhil

Report no : 2024.099
Coach : Dr. Giovanni Bordiga
Professor : Dr. Davood Farhadi
Specialization : Mechatronic System Design
Type of report : Master's Thesis
Date : November 27, 2024

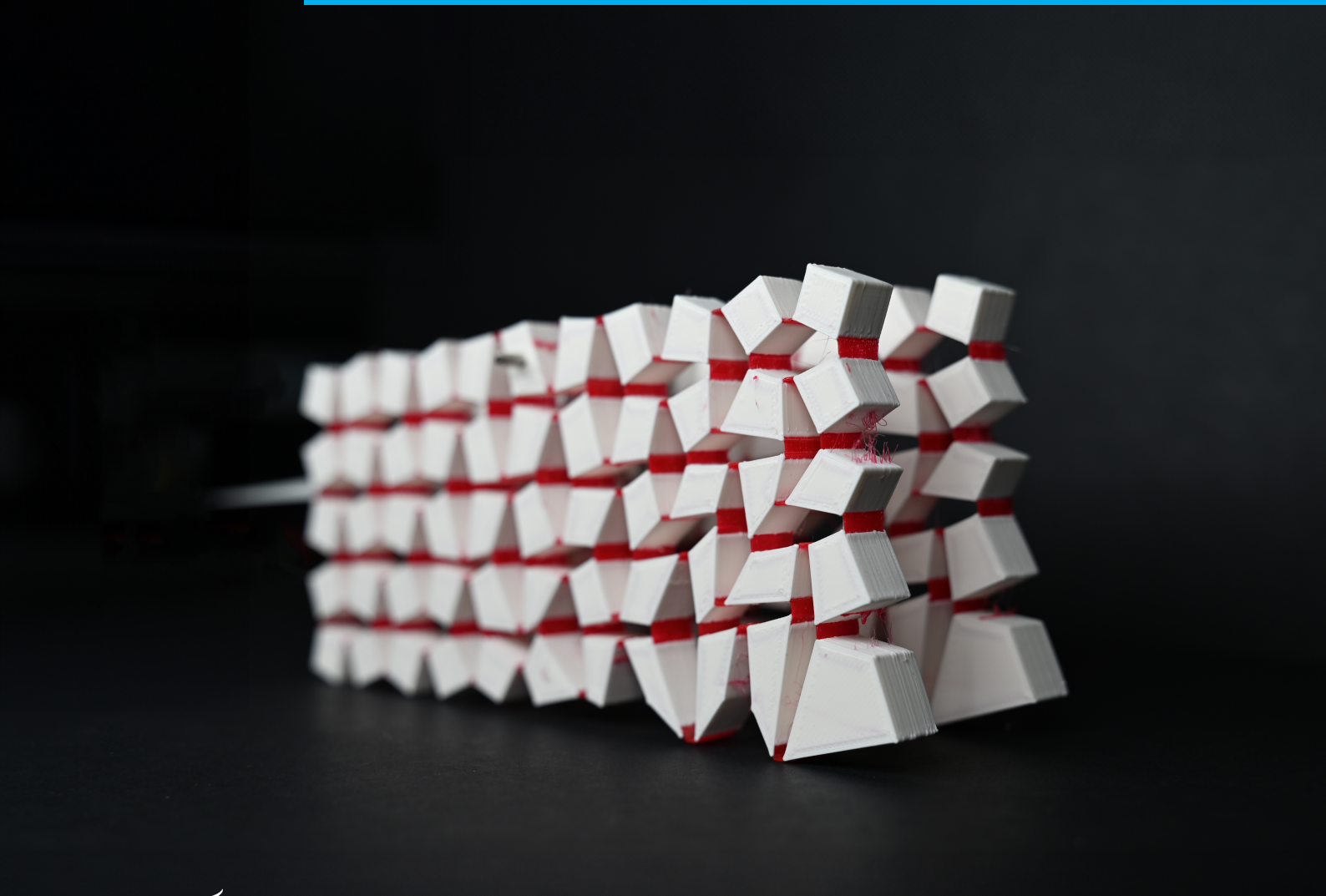

Dynamic Mechanical Metamaterials for Path Generation

Master's Thesis

by

Tom Vreugdenhil

Student High-Tech Engineering
Delft University of Technology, The Netherlands

Student number:	4720385
Project duration:	November 2023 - November 2024
Thesis committee:	Dr. Davood Farhadi, supervisor TU Delft
	Dr. Giovanni Bordiga, supervisor Harvard
	Dr. Farbod Alijani, external examiner TU Delft

Acknowledgements

The past years at TU Delft, beginning with my bachelor's, through my Dream Team experience, and now culminating with my master's, have been incredibly rewarding. These years have shown me what a privilege it is to study at one of the world's premier technical universities, and they have led me to this final milestone—my thesis. I want to acknowledge the invaluable contributions of many people who have supported and guided me along the way.

First and foremost, I would like to thank my TU Delft supervisor, Dr. Davood Farhadi, for his insightful guidance and support throughout this thesis. I am grateful for the opportunity he provided to explore a research topic that perfectly aligns with my interests in dynamics and compliant mechanisms. I am also deeply thankful to Dr. Farhadi for introducing me to the Bertoldi Group at Harvard, which allowed me to spend six unforgettable months abroad. My time at Harvard gave me a chance to study in a remarkable academic setting and to explore the vibrant city of Boston.

At Harvard, I was fortunate to have Dr. Giovanni Bordiga as my daily supervisor. I am sincerely grateful to him for his availability, open discussions, and his introduction to the field of mechanical metamaterials. Working with Dr. Bordiga has been a wonderful collaboration, and I could not have asked for a better colleague. I would also like to thank Professor Katia Bertoldi and all of her group members for their warm welcome, guidance, and for the enriching discussions that helped shape my research.

To my friends and my girlfriend, who felt so far away when I was in Boston, thank you for your support and love. You helped me through the more challenging days and reminded me of home.

Lastly, and most importantly, I want to thank my parents. Their unwavering support throughout my studies at TU Delft has been my foundation. I am incredibly grateful for their encouragement, which allowed me to study abroad, and for everything they have done to help me become the engineer I am today.

This thesis is as much a reflection of their influence and encouragement as it is of my own efforts. Thank you all for being part of this journey.

Contents

Preface

The thesis you are reading studies a fascinating subject; the ability to achieve material performances beyond what can be found in our green earth: metamaterials. These structures exist at large and small scales and can provide properties previously unknown in regular materials. While it is still undergoing research, and few applications truly exploit what metamaterials can offer, I hope this thesis provides a glimpse of what is possible with metamaterials and their possible applications and motivates you, the reader, as much as me.

The structure of this thesis is the following. First, section 1 introduces the subject and delves into the primary research, focusing on the identified knowledge gap in the field and exploring the integration of path-generating metamaterials. Subsequently, section 2 presents a comprehensive review of the relevant literature, which was done in the first stage of this thesis, on path generation and mechanical metamaterials, outlining the state-of-the-art in these areas. Finally, section 3 includes supplementary information, offering detailed insights and supporting data throughout the thesis.

1 Paper

This section presents the main research paper for the thesis. It introduces the topic, the existing state-of-the-art, and the methods. The result: a robotic walking prototype, and its limitations and future advancements are discussed.

Dynamical Mechanical Metamaterials for Path Generation

Tom Vreugdenhil[a,b]

[a] Precision and Microsystems Engineering, Delft University of Technology, Mekelweg 2, 2628 CD Delft, The Netherlands ; [b] John A. Paulson School of Engineering and Applied Sciences, Harvard University, Cambridge, MA 02138, USA

This manuscript was compiled on November 13, 2024

Many robotic applications require moving an end-effector through intricate closed-loop paths for object manipulation or locomotion. Conventionally, rotary-actuated rigid-link mechanisms perform this task successfully. However, several drawbacks, such as wear, play, and assembly difficulties, limit their performance. In high-speed applications, these rigid and often bulky links require high accelerations, leading to high power usage or the need for dynamic balancing, further complicating the mechanism. Rigid mechanisms are not the only ones that generate paths; compliant mechanisms are also widely used. However, compliant hinges cannot undergo complete rotations by definition, making cyclic actuation impossible. As a result, creating closed-loop paths typically requires multiple actuators—one per end-effector degree of freedom—adding to power demands and complexity. In contrast, closed-loop deformations can occur when dynamically actuating a soft body with a single actuator. We can create customizable soft bodies that leverage internal dynamics by structuring this soft body with a mechanical metamaterial made of tessellated compliant cells and designing its internal geometry. This research explores how these dynamics can be harnessed for path generation within mechanical metamaterials. Through multi-objective optimization, we embed reprogrammable control strategies within the metamaterial geometry, enabling adaptive responses to actuation frequency and amplitude for complex behaviors. We validate these designs with tabletop prototypes, building up to a self-propelled, walking prototype—a step toward autonomous robotic metamaterials. Future advancements include optimizing for propulsion and adaptability to create versatile, self-propelling robotic metamaterials. Embedding multi-objective control into the geometry could allow a single design to perform multiple functions based on actuation or external influences. This approach holds promise for new adaptive capabilities in robotic metamaterials.

metamaterials | path generation | dynamics | optimization

Introduction

Path generation is central in industries focused on precise object manipulation and automated movement, from robotic arms to autonomous transport systems [1]. Conventional approaches rely heavily on rigid-link mechanisms, which use rigid links and joints to transform motion into designated output paths (Figure 1), such as those generated by four-bar linkages [2]. However, these systems fall short under real-world conditions. They are prone to alignment issues, mechanical wear, and complex manufacturing and assembly requirements [3], which significantly constrain their adaptability in generating complex, multi-directional paths. Attempts to improve path generation by replicating these rigid mechanisms with pseudo-compliant systems [4] [5] are again limiting, often originating from binary topology optimizations [6] and struggle with high-speed applications and vibrations that disrupt performance.

This study introduces a new direction in path generation by shifting to mechanical metamaterials, materials engineered to have unique properties beyond those found in nature [7], which enable dynamic path generation that is reprogrammable with a single actuator (Figure 1). This approach significantly diverges from rigid or quasi-compliant mechanisms, since our metamaterial gains control over the generated path's degrees of freedom (DOFs) [8] through underactuation [9] and internal dynamics. Underactuation means purposely actuating the system's input with fewer degrees of freedom than the output or endeffector will give [10]. Rather than relying on multiple actuators or fixed path geometries, our metamaterial design harnesses internal dynamics to adaptively generate multiple paths in response to a single, simple back-and-forth input. This strategy provides reprogrammability and versatility that existing approaches cannot match, especially in high-speed applications. Previous studies laid the groundwork by examining quasi-static metamaterials for path generation [11], metamaterial mechanisms [12], and dynamic metamaterials for energy focusing [13]. All are fundamental platforms with the freedom of finding a metamaterial structure capable of a specific function systematically instead of thinking of a structure with intuition [14]. However, none have achieved the combination of single-input control and dynamic reprogramming we present here. Our work fills this critical gap, demonstrating how mechanical metamaterials, configured as blocky structures driven by rectilinear input, produce multiple paths—without additional actuators, external influences, or physical changes. Metamaterials and compliant mechanisms are inherently limited to rectilinear actuation instead of rotary [15]; however, exploiting metamaterial elasticity provides the solution in our case. This adaptability allows our system to generate different outputs, such as robotic walking gaits or

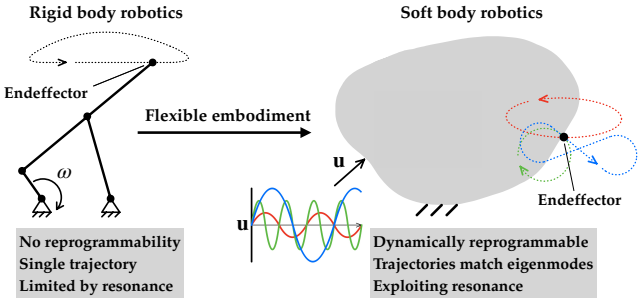

Fig. 1. Rigid and soft robotics comparison: Overview and comparison between some generic rigid-link mechanism and its envisioned soft matter counterpart with yet unknown shape, size, and internal structure.

reconfigurable trajectories with the same metamaterial structure. This significantly advances quasi-static or multi-actuator designs in simplicity, doing more with less.

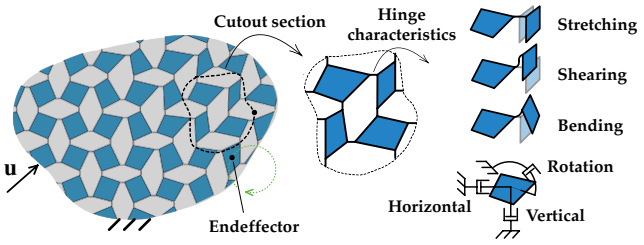

Fig. 2. Proposed soft embodiment: Soft embodiment with an internal blocky metamaterial lumped compliant structure, random geometry, and hinge stiffness and damping characteristics.

In this study, we develop a blocky metamaterial system comprised of rigid, four-cornered units connected by elastic elements at each corner (Figure 2). Each elastic component contains uncoupled stiffness and damping properties. By optimizing this structure, through automated differentiation [16], to respond predictably to a single input, we achieve a system capable of reprogramming its path dynamically. The results section explores sensitivity and robustness, presents a streamlined fabrication method to mitigate manufacturing errors, and the straightforward assembly of a robotic prototype. Through experiments, we validate the metamaterial's ability to generate multiple paths and demonstrate its potential to create multifunctional outputs, obtaining reprogrammability and tackling limitations that rigid systems face at high speeds. Our findings point toward a future where mechanical metamaterials redefine path generation by harnessing inertia and reprogrammable paths through a single, straightforward input. We conclude with insights into the broader implications of this approach, emphasizing how it could disrupt traditional path-generation paradigms and redefine the design of underactuated robotic systems.

Methods

A metamaterial design platform alone does not suffice; it leaves the road toward path-generating mechanisms unexplored. Although energy-based approaches form the backbone of this framework, optimizing solely for energy accumulation or dissipation does not directly contribute to path-generating metamaterials. We investigated how to translate a target path into an objective function, capturing any parametrized shape with precision points in a specific order to control directionality throughout the trajectory. After the equations of motion are solved, we calculate how well the generated trajectory matches the target trajectory. From the start, we understand that choosing the right constraints and actuation type will help the optimization reach a good result. Yet, the availability of every block in the metamaterial makes this impactful choice even more challenging. Additionally, we developed a more intricate actuation method for the metamaterial aimed at a robotic prototype, where the actuator moves within the same inertial frame as the metamaterial rather than remaining stationary during experiments. Once we landed on a promising simulation result, we evaluated the design's robustness to variations in actuation and random manufacturing errors. If the design proves effective, we manufacture it using a specialized dual-material 3D printing technique, embedding flexible hinges in rigid blocks to create a robust, near-monolithic prototype free of manufacturing errors.

Endeffector dynamical response. In Figure 3, geometry ($\boldsymbol{g}$) which are the coordinates of the $j = 1, ..., 4$ corner nodes of the $i = 1, ..., n$ units and actuation parameters A and $\omega = \frac{1}{f}$ ($\boldsymbol{a}$) combined provide the necessary information to solve the earlier mentioned equations of motion (solving the forward problem, as depicted in Figure 3) and lead to finding the dynamical response ($\boldsymbol{q}$). Path generation requires an endeffector, the point on a mechanical system that traces the desired path. This intuitive choice avoids additional overly complex discrete optimization processes [17] that would overburden an already intensive gradient-based optimization. Knowing the dynamical response of the entire metamaterial allows for extracting the coordinates of the chosen end effector over time. Since the actuation input is inherently cyclic in time, the endeffector will show a limit cycle in absence of chaos. Therefore, only the final cycle in the simulation is extracted and compared to a target trajectory with an equal number of target points to overcome frequency multiplications between input and output. Evaluating every target point compares the coordinates while restricting position and timing. Calculating the cumulative deviation between endeffector and target points using the l^2-norm [18] results in an error of units $[mm]$, defined as the cost function ($\boldsymbol{C}$) where n is the number of target precision points.

$$C = |c_{tot}| = \sqrt{\sum_{i=1}^{n} c_i^2} \tag{1}$$

Updating the metamaterial design. Cumulative cost functions for the endeffector are now in place and with the use of automatic differentiation [16], gradients of the cost function to all geometrical design variables (the four corners of every unit) and, if desired, to the actuation parameters can be calculated efficiently (Equation 2).

$$\frac{\partial C}{\partial g} = \frac{\partial C}{\partial q}\frac{\partial q}{\partial g} \qquad \frac{\partial C}{\partial a} = \frac{\partial C}{\partial q}\frac{\partial q}{\partial a} \tag{2}$$

Once calculated, the gradients are fed to an optimizer which applies the Method of Moving Asymptotes (MMA) (from the NLopt library) [19] and updated design variables refresh the geometry and actuation. This cycle repeats until convergence criteria come into play and end the optimization.

Manufacturing and testing. Optimized geometries are manufactured for testing using 3D printed Polylactic Acid (PLA) [20] for the rigid units. Prior work by *Bordiga et al.* manually inserts thin polyester plastic shims to act as hinges between rigid units. After replicating this method, it easily led to manufacturing errors, and the manual labor was time-consuming. The hinges can also be 3D printed similarly to the PLA rigid units but with a flexible material such as Thermoplastic Polyurethane (TPU) [21] (see SI section 5). By subsequently printing PLA, leaving open a small slit, and filling this slit with TPU layer by layer, the hinge is fully constrained within the PLA unit (see Figure 4). With this, we mitigate the influence of human error, and manufacturing errors are within machine precision [22]. No further post-processing is required,

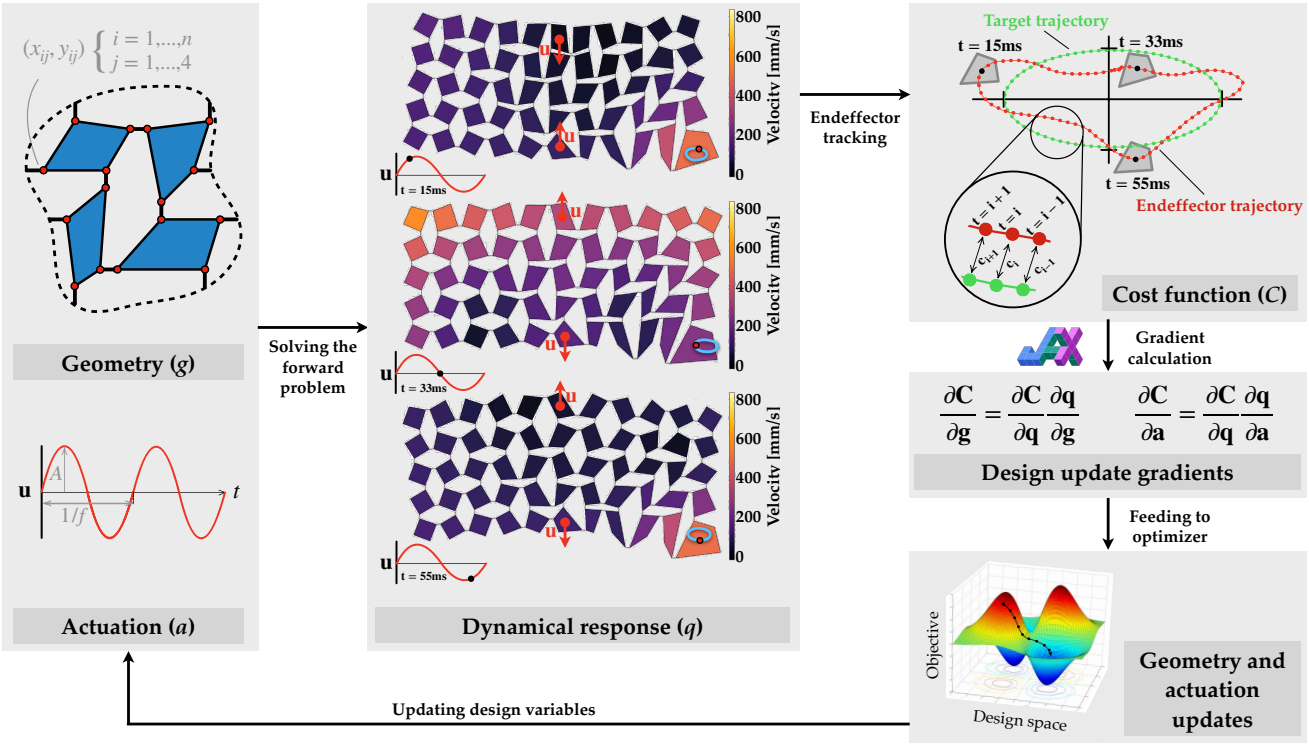

Fig. 3. Optimization cycle for path generation: Overview of the optimization scheme, with geometry (***g***) and actuation parameters (***a***) as possible design variables, dynamical responses (***q***) and endeffector trajectories as output information and at last calculation of cost function (***C***) and gradients towards design variables leading to updates in design variables through an optimizer.

and the printed specimen will be fully ready after printing if there are no printing defects. By elevating the prototype in the horizontal plane and constraining the necessary blocks to match the optimization, a deformation input $(\omega, A)_{design}$ is applied using a shaker. The dynamical response is captured using high-speed video recordings and post-processed with tracking software to extract the true endeffector trajectory to compare with the simulations.

Results

With a working optimization and manufacturing strategy, the capabilities of the computational model are investigated. Exploring these capabilities means choosing the number of rigid units in the horizontal and vertical direction, which units should be constrained and how, which unit to actuate, and finally, where should the endeffector be. The answers to these questions came by intuition to omit discrete optimizations. Sizewise, the horizontal and vertical number of units corresponds to what can be 3D printed on a regular print bed of 200x200mm [22], resulting in 13 units horizontally and 7 vertically. This configuration allows for many design variables, hence a large design domain. Actuating and constraining go hand in hand, requiring a smart solution to not (locally) overconstrain the metamaterial, leading to a stiff system where it is difficult to obtain reasonable endeffector displacement. This smart selection involves positioning the constrained and actuated units away from the end-effector. The constrained unit can be placed at a corner or in the middle of any side (as shown in Figure 5). In contrast, the actuated unit is located at a corner or middle of another side, leaving the end-effector positioned in any remaining corner. Finding out what kind of endeffector paths were possible with this framework meant specifying several target shapes and sizes. We tried different constrained and actuated units combinations, presenting some of the best results in Figure 5.

Figure of eight path. The figure of eight is a shape consisting of two semi-circles with a crossing in the middle and parametrized in x and y coordinates as such:

$$x(\theta) = r_a \cos(\theta), \;\; y(\theta) = r_b \sin(\theta)\cos(\theta), \;\; 0 \leq \theta \leq 2\pi \qquad (3)$$

where r_a and r_b correspond to the major and minor radii, respectively, chosen to be 10mm and 5mm. Changing the order of theta gives control over the direction of the actuated path; in this case, the order is unmodified. The actuation input is applied vertically to the top left unit $(\omega, A)_{in} = (20[\text{Hz}], 7.5[\text{mm}])$ and after optimization updated to $(\omega, A)_{opt} = (19.40[\text{Hz}], 13.62[\text{mm}])$, the top right corner and lower middle units are fully constrained in horizontal, vertical and rotation directions. The endeffector is in the lower right corner.

After a successful optimization, the optimized geometry and endeffector trajectory is given in Figure 5 (**A1** and **B1**). Visually, the endeffector trajectory matches the target trajectory well in size, shape, and location of the intersection. As denoted by the opacity of the blue line, the result quickly converges to a limit cycle. Mathematically, the cumulative l^2 error (Equation 1) comes down to $\sim$ 5mm spread over 51 data points, thus a pointwise error of $\sim$ 0.1mm.

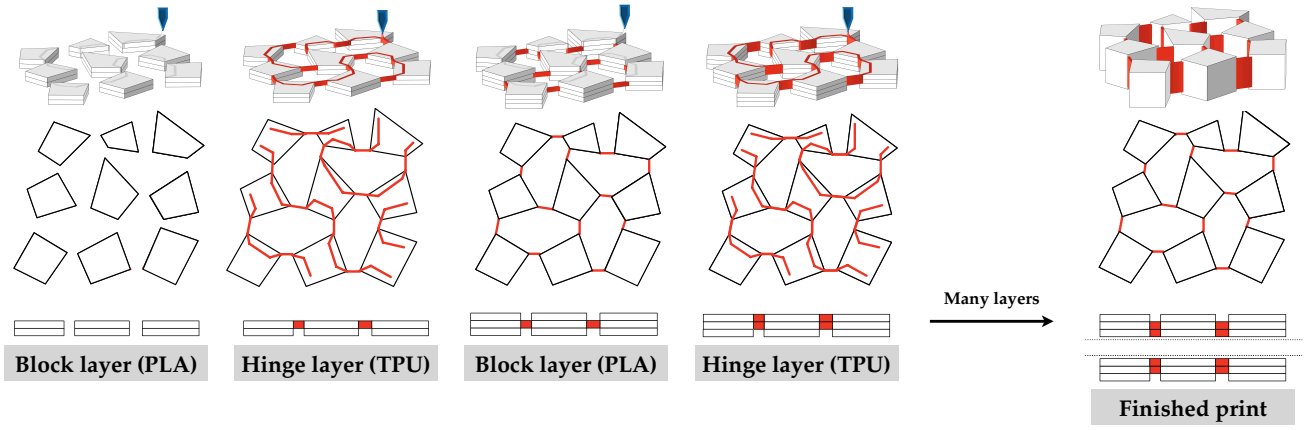

Fig. 4. Manufacturing process: Double filament (PLA rigid units and TPU flexible hinges) 3D printing scheme to facilitate the production of mechanical metamaterials with adequately compliant hinges with respect to the rigid units while upholding the need for a single-part finished product without manual manufacturing steps.

Evaluating the influence of actuation parameters ω and A meant simulating the optimized design at frequencies and amplitudes around the optimal solution. We construct the range of simulated amplitudes and frequencies with steps of $0.1A_{\text{opt}}$ and $0.1\omega_{\text{opt}}$. Using these ranges, we simulate every possible combination of frequency and amplitude, and we show a random selection of points and their trajectories in Figure 5 (**C1**). This figure clearly shows a narrow near-vertical white band, meaning two things: the optimized design is less sensitive to amplitude than it is to frequency. This sensitivity is shown even better by the sharp increase in greyscale left and right from the near-vertical band where cumulative l^2-errors quickly climb from $5-10$mm to $20-60$mm. Clearly visible is the cause for an increase in overall size, which is the amplitude. This increase is obvious when comparing the trajectories in the lower left ($\sim$ 17.50 [Hz] and 11.5 [mm]) and middle top ($\sim$ 19.50 [Hz] and 15.00 [mm]). Next to size differences, the influence of frequency is observable, especially when looking at lines perpendicular to the frequency axis. The greyscale aggressively changes in this direction with changes in trajectory quality while respecting the main dimensions (r_a and r_b) of the figure eight trajectory.

Sensitivity towards geometry gives information on whether manufacturing errors ruin the endeffector trajectory's quality. A small random error (as defined in Equation 4) is applied to the coordinates of all four corners of all units in the metamaterial (blue geometry in Figure 5), shifting each corner and creating a changed geometry (green geometry in Figure 5). Interestingly, error factors up to ~ 0.3 still create trajectories with an l^2-error of $\sim 10-15$mm. Only afterward, with error factors ≥ 0.3, l^2-errors skyrocket, and visually, the trajectory does not make sense anymore.

$$(x_{ij}, y_{ij})_{rnd} = (x_{ij}, y_{ij})(1 + e_f R), \text{ where } R \sim U[-1, 1] \quad (4)$$

We calculate the dynamical response for each error factor and plot its final trajectory with the error factor on the horizontal axis and the corresponding l^2-value on the vertical axis. Geometrical errors do not influence the important qualities of a trajectory much; its overall size, shape, and direction remain virtually untouched for an error factor between 0 and 0.2. An interesting remark here is the consistent placement of the crossing within the figure eight trajectory. Only after error factors of 0.25 and higher, the crossing starts to shift, and the ratio $\frac{r_a}{r_b}$ gets worse with scaled or skewed trajectories as a result.

Horizontal ellipse path. The horizontal ellipse is oval-like and parametrized as such:

$$x(\theta) = r_a \cos(\theta), \; y(\theta) = r_b \sin(\theta), \; 0 \leq \theta \leq 2\pi \quad (5)$$

where r_a and r_b correspond to its major and minor radii, 10mm and 5mm respectively. Theta is again unmodified, which means oriented counterclockwise (CCW). The middle block in the top row is vertically actuated with $(\omega, A)_{in} = (20[\text{Hz}], 7.5[\text{mm}])$ and after optimizing $(\omega, A)_{opt} = (20.23[\text{Hz}], 8.59[\text{mm}])$. Only the lower middle block is constrained, and the endeffector is in the lower right corner.

After optimization the geometry updated to Figure 5 **A2** with trajectory **B2** as a result. Directionality, size, shape, and overall positioning obey well with a resulting l^2 error of $\sim$ 5mm on the final trajectory.

In terms of sensitivity towards actuation parameters ω and A, Figure 5 **C2** shows oval-like greyscale lines nearby the optimized actuation parameters ($(\omega, A)_{opt}$) indicating the almost equal importance of amplitude and frequency. Similar to the figure eight, amplitude mainly influences the overall size or captured area. The frequency is a squared term in the kinetic energy ($E_k = \frac{1}{2}mv^2$) and, therefore, manipulates the quality of the created trajectory, or the ability of the trajectory to match the target parameters r_a and r_b.

Simulating the metamaterial with random geometrical errors, similarly as before, shows the importance of manufacturing errors as depicted in Figure 5 **D2**. There is good robustness, as the overall result stays mostly intact for geometrical error factors up to 0.2, meaning a 20% error in the coordinates of each unit in its optimized state, while only increasing the l^2-error from ~ 5 to ~ 10 mm. This is a 200% increase in absolute error, but the error response visually does not influence the trajectory much. Only with geometrical errors above 0.25 the l^2-error ramps up quickly, after which even larger errors cause the cost value to increase to a poor trajectory.

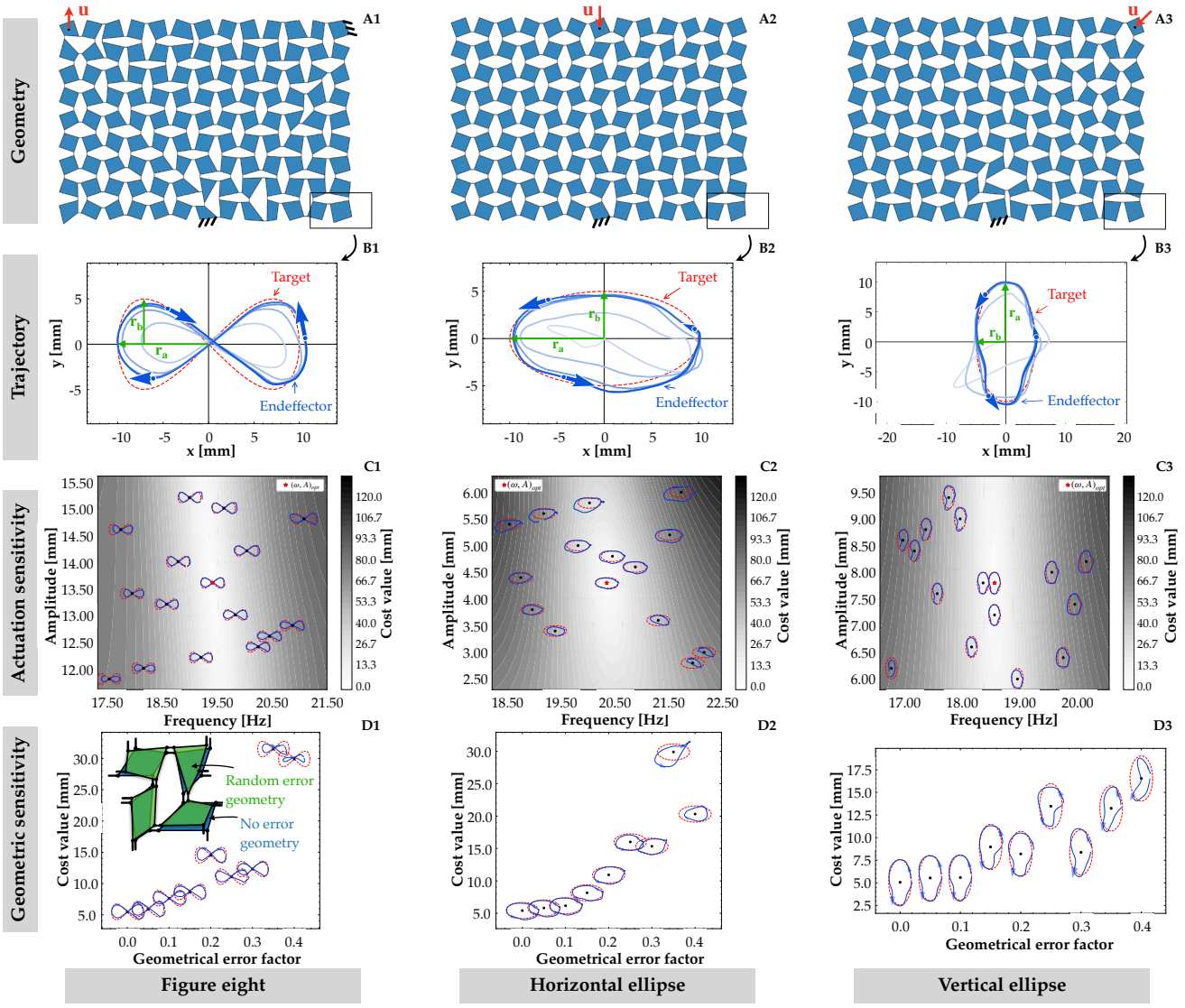

Fig. 5. Optimization results of three successful optimizations on a 13x9 units mechanical metamaterial (**A1**, **A2**, **A3**) with each a different target trajectory: figure eight (**B1**), horizontal ellipse (**B2**) and vertical ellipse (**B3**). Sensitivity towards actuation frequency and amplitude are given (**C1**, **C2**, **C3**), and robustness towards a random error in nodal geometry (**D1**, **D2**, **D3**) is shown for each result.

Vertical ellipse path. The vertical ellipse is oval-like and parametrized as such:

$$x(\theta) = r_b \cos(\theta),\ y(\theta) = r_a \sin(\theta),\ \ 0 \leq \theta \leq 2\pi \qquad (6)$$

Both radii are flipped with respect to the prior horizontal ellipse, meaning r_a and r_b correspond to 5mm and 10mm. Directionality is unchanged, meaning counterclockwise. The metamaterial is actuated at the top-right corner with an angle of 45 degrees (to the horizontal) while keeping the lower middle unit constrained. This interesting combination of actuating and constraining comes from a trial-and-error approach to finding the best-performing design. Similarly to the figure eight and the horizontal ellipse, the bottom right block is the endeffector. Actuating initially happens with $(\omega, A)_{in} = (20[\text{Hz}], 7.5[\text{mm}])$ and after optimizing ends up at $(\omega, A)_{opt} = (18.68[\text{Hz}], 15.50[\text{mm}])$.

Optimizing this system results in a changed geometry as shown in Figure 5 **A3** with an interesting remark. The left half of the metamaterial remains fairly unchanged from the original structure. This part of the design space does not contribute much to the objective but acts as a counterweight. Figure 5 **B3** shows some deviation in the generated trajectory with respect to the target but still has a final l^2 error of $\sim$ 5mm.

Similar to the results for the figure eight, and contrary to the similarly-shaped horizontal ellipse, the sensitivity shows a narrow vertical band near the optimized design point ($(\omega, A)_{opt}$). From this, it is clear that the actuated frequency is the dominant factor and that, within the investigated range, the amplitude is of little influence on the trajectory quality. We see that along the frequency axis, the optimized trajectory loses its ability to match r_a and r_b. In contrast, along the amplitude axis, the ratio of r_a and r_b remains fairly constant; the trajectory looks similar but increases or decreases in overall

size.

Geometrically, the vertical ellipse is inherently slightly deviating from the target. This trend is amplified by increasing the geometrical errors and simulating the system, and error factors of just ~ 0.1 narrow the ellipse to obtain foot-shaped trajectories. Furthermore, with error factors above 0.1, the result does not resemble an ellipse anymore as the ratio between r_a and r_b worsens (l^2 errors of ~ 10mm) and also leads to a visually bad result, something that the horizontal ellipse did not have to such extend.

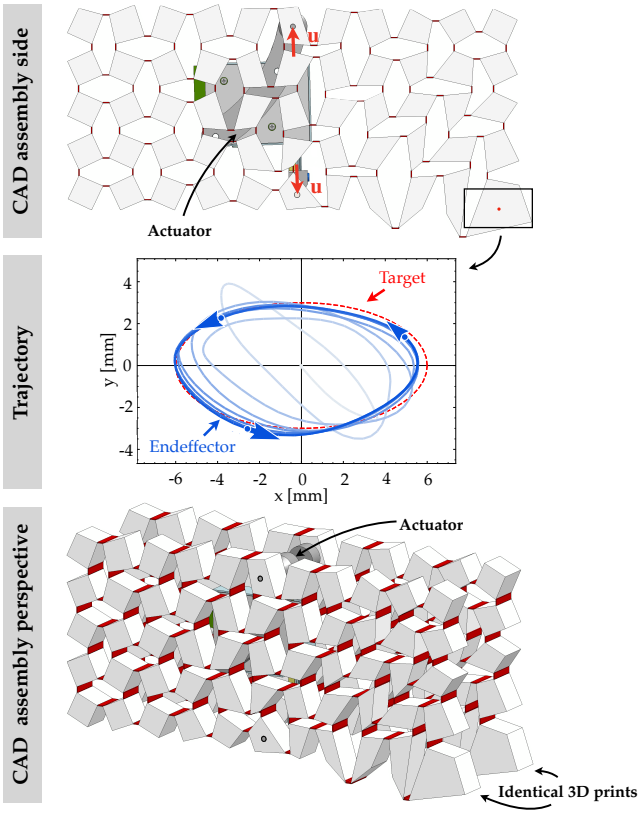

Fig. 6. Assembled CAD prototype and optimized trajectory: CAD assembly of robotic metamaterial prototype with the mounted actuator in side view, the generated endeffector trajectory, and the assembly in perspective

Case study: robotic metamaterial with walking gait. Path generation in mechanical metamaterials is possible. From here on, this ability transforms into a more intriguing application of a robotic metamaterial capable of performing a walking gait. For stability reasons, two identical metamaterials are assembled some distance apart (Figure 6), and an actuator in between to actuate both metamaterials simultaneously. The robotic metamaterial consists of eleven units horizontal and five units vertical (11 by 5); this size has good enough dynamic deformation at the endeffector while keeping the overall size to a minimum such that the actuator could actuate two metamaterials in parallel.

For a walking gait, we select the horizontal ellipse (Equation 5) as it already mimics a walking motion and works well in the simulations. In terms of size, the horizontal ellipse contains $r_a = 6$mm and $r_b = 3$mm to account for the smaller number of units and overall size of the physical metamaterial. Actuation happens in a more specific way, as a body-mounted actuator (SI section 1) [23] moves with the body. Body-mounting happens so that any two units will move co-linearly towards and apart from each other, unaffected by how the metamaterial dynamically deforms. This approach effectively replicates the actuator instance, as if there is an imaginary massless strut with time-dependent length between the actuated units' centroids. These actuated blocks can rotate along their centroid, through which the actuator acts, to reduce constraining forces. The top middle and bottom middle blocks are actuated in this case study to place the actuator approximately in the centroid of the metamaterial. The only constraint keeping the system in place during simulations is fixating the center of the earlier mentioned imaginary strut in horizontal and vertical directions while leaving rotation free. In the lower right corner of the metamaterial we place the endeffector, and, aligning with the actuator specifications, the input actuation is $(\omega, A)_{in} = (14.00[\text{Hz}], 2.0[\text{mm}])$, after optimizing this ends up as $(\omega, A)_{opt} = (15.35[\text{Hz}], 2.0[\text{mm}])$. Due to actuator limitations, the input signal is not a true sinusoid but a piecewise linear approximation with a sawtooth signal. The maximum and minimum values of the sawtooth align with the amplitude of the sinusoid, and the crossings at $t = 0$, $t = \frac{T}{2}$ and $t = T$ align with the frequency of the desired sinusoid.

After optimization, the geometry (as in the top row of Figure 6) contains an endeffector that has evolved into a larger high-mass unit. A high mass is beneficial for focusing on kinetic energy, and its neighboring units are slender, giving the endeffector the required displacement freedom. The created endeffector trajectory (Figure 6) is accurate and resembles the target trajectory well (l^2-error of ~ 4mm). Next to accuracy, the endeffector quickly spirals towards the target limit cycle. Together with the actuator, we manufacture the metamaterial with the 3D printing method explained in Figure 4 and assemble it in a few simple steps (SI Figure 3). Figure 6 presents the final prototype, with more detailed pictures in SI Figure 4.

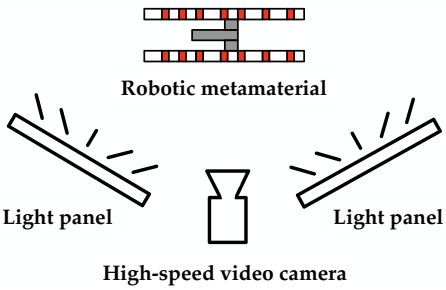

Fig. 7. Schematic top view of the experiment setup: On top, the robotic metamaterial, left and right the light panels, and a high-speed video camera.

Verifying whether this robotic metamaterial works meant performing two types of experiments: the scenario where the complete assembly is floating without friction or normal forces, and the scenario where the robotic metamaterial is placed on the floor to see its walking capabilities.

Figure 7 shows the experimental setup schematically where the robotic metamaterial stands in front of a camera. By clamping the actuator body, the endeffector can move freely, but additional boundary conditions are applied, creating a scenario not captured by the optimization. Now, the top actuated unit is constrained to a simple pin joint, and the bottom

unit is an actuated pin joint moving linearly in the direction of the top joint with a sinusoidal signal (top row in Figure 9). The result of the experiment is the blue trajectory, and in red the simulation predicts this specifically constrained scenario. Immediately, it is clear that the model is sensitive to different boundary conditions for the same optimized geometry, as the model simulation shows extensive deformations while the experiment is generally correct in size but not in shape compared to the target ellipse. On the other hand, the orientation of both simulation and experiment do align.

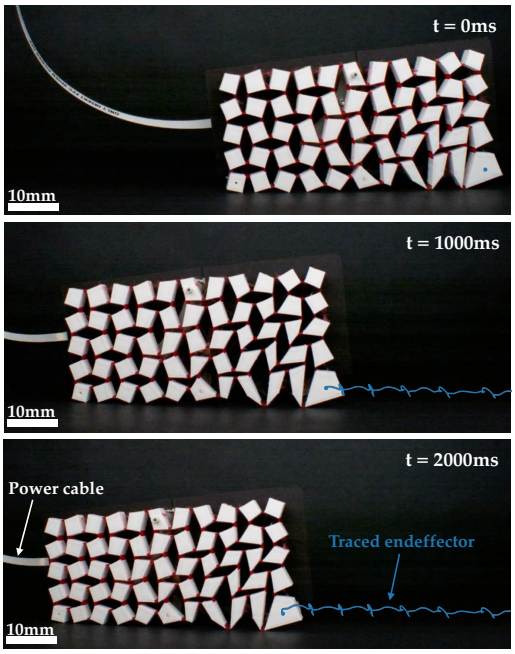

Fig. 8. Robotic walker snapshots from the experiment in contact with the floor: Three snapshots from $t = 0ms$ to $t = 2000ms$ of the conducted experiment with a free-moving robotic metamaterial. The blue line indicates the traced endeffector trajectory to show the influence of floor contact, friction, and normal forces.

Experiments in the real world scenario show interesting results too. The prototype is on the floor, where normal forces and friction come into play; both factors are not considered during optimization to investigate the model's capabilities without overcomplicating it. As explained in the case study, the actuated units always move towards each other to simulate as if there was a physical actuator in between them (see second row in Figure 9). The result highlights the enormous influence of normal and friction forces, as the demolished trajectory shows. The simulation without normal or friction forces shows the red trajectory, where the metamaterial floats in space with only the actuator (or imaginary strut) constrained in the horizontal and vertical directions. This simulation is identical to the optimization model, meaning the endeffector trajectory it generates is the optimized and desired result. However, external forces constrain the dynamics of the endeffector to such an extent that the inertial forces of the metamaterial cannot overcome them with diminished trajectories as a result, even though directionality is correct (blue trajectory in the second row of Figure 9). Interestingly, when analyzing the global motion of the prototype, the snapshots in Figure 8, the direction in which it propagates aligns with the direction of the walking gait (counterclockwise or to the left). The blue line indicates the traversed path of the endeffector in its local walking gait on top of the global motion; this shows smaller steps than simulated due to the external forces acting on the endeffector and other points in contact with the floor, suppressing the trajectory.

Discussion

The results in Figure 9 give a good insight into the model's performance without adding complexity regarding external forces and the trajectory's sensitivity towards different boundary conditions. Initially, the idea was to simulate the robotic metamaterial as accurately as possible to the real scenario without introducing external forces and evaluate the model with no additional complexity. This meant creating the imaginary strut actuation method, where two units always move in the direction of the line through the centroid of these units. By constraining this imaginary strut's horizontal and vertical displacement (leaving the rotating DOF free), the computational model did not fight against global displacements, causing the whole metamaterial to drift and lose control over endeffector accuracy. In reality, this is not a problem, and actually, the reason for creating a robotic prototype is to prove that path generation could be a foundation for creating propelling robotic gaits. On the other hand, this research initially started with path generation. The experiment should constrain the metamaterial to stay in the camera's frame to evaluate the trajectory accuracy. This means fixating the actuator in a similar sense. Since the imaginary strut varies in length and can rotate, this led to near-impossible capturable constraints in reality, as the actuator will always actuate one point relative to another. In other words, it has a fixed part and a moving part. Simplifying this led to constraining the fixed part of the actuator, knowing this is also the high-mass part of the actuator and leaving the moving part to actuate the prototype. This results in the scenario in the top row of Figure 9 with a floating metamaterial and a fixed actuator.

Secondary to using constraints that align with reality and fit the current computational model, the choice of where the endeffector should be is nontrivial. Since any geometry can be optimized, any choice of endeffector can work, though to what extent cannot be known exactly prior to optimizing. Making a smart decision, therefore, came down to evaluating endeffector choices with unoptimized geometry on their dynamic deformation. It is a suitable candidate if a certain trial-and-error combination of constraints, actuation, and endeffector resulted in deformations in the same order of magnitude as a target trajectory. The best choice would be to include the endeffector choice as a design parameter. However, this introduced such immense discrete optimizations surrounding the existing optimization that the trial-and-error selection method seemed reasonable. The choice is important, especially when thinking about a robotic metamaterial, where the endeffector will be in contact with external objects such as the floor. The current model used the centroid of any unit as an endeffector instead of the anticipated contact point (corner of a rigid unit). Exploring the corner point as an end effector typically results in many high-order fluctuations and vibrations in the trajectory; this led to poor outcomes, which the centroid did not show often. Altogether, the centroid of an endeffector is still close to being in contact with the floor that, as long as the endeffector does not rotate substantially, its rigid-body motion

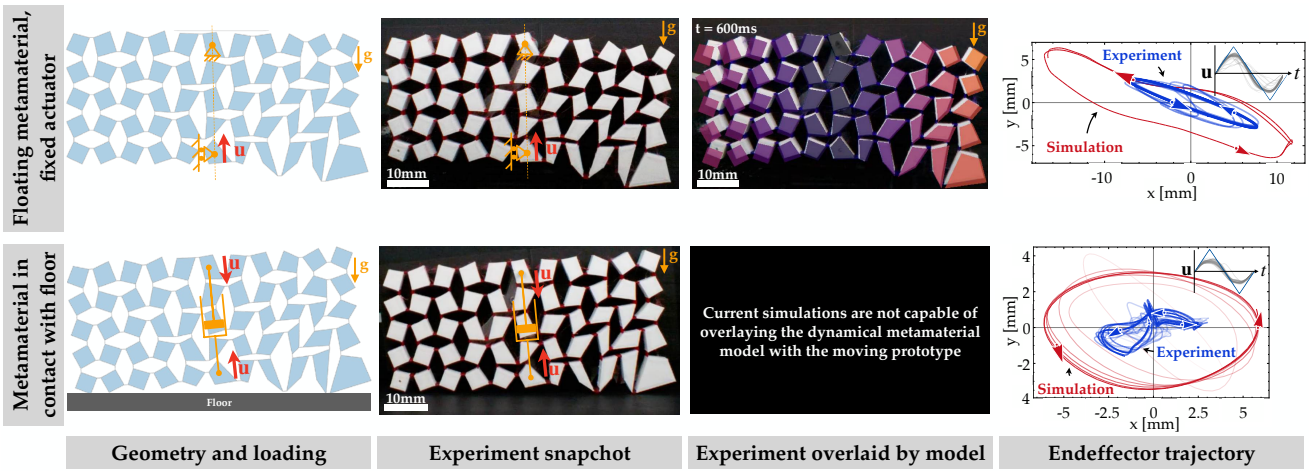

Fig. 9. Two conducted experiments on a robotic metamaterial with walking gait: Results of two types of experiments on the robotic metamaterial with walking gait, with a clamped actuator and a single moving unit (first row) and without any constraints (second row) where the piston indicates the type of actuation in between two units. The first column presents the optimized geometry and constraints schematically; the second column shows an experimental snapshot with schematic constraints; the third column displays an overlaid simulation snapshot; and the last column compares the generated trajectory with its traced input signal to the perfect signal.

would still represent a walking gait at the contact point with the floor, especially once individual units can be scaled down. Applying the constraints similar to how the experiment was conducted results in a metamaterial hugely overestimating the experiment trajectory. Most probably, this is due to stiffness and damping characteristics (Figure 2) in the model (see SI section 4). By rescaling the simulation deformations, a more reasonable response can be obtained (see SI Figure 12). There, the deformation is scaled by $x0.5$, and the shape, orientation, and direction of the trajectories match well, leading to a suspicion about the model characteristics and its performance in a steady state dynamic simulation, contrary to just transient dynamics [13]. Possible higher-order stiffness terms to account for nonlinearities in geometry and viscoelastic stiffness in the TPU material for the hinges could resolve this issue. Next to improving these characteristics, the objective function to obtain a certain path can also be rethought. The used l^2-norm constrains precision points in a trajectory in position and time ($[x, y]_i(t)$). In the case of just path generation, where endeffector velocity is not important, the timing constraint may impede the search for a good solution. The design domain increases substantially by releasing a timing constraint, where the endeffector can obtain any velocity throughout the trajectory. No control over velocity has strong drawbacks in path generation and robotic applications. A mechanism where this alignment timing is unknown or has a large variance most certainly introduces a failure. Though each application is specific, an increase in trajectory accuracy by removing timing constraints could be worth the cost of losing control over velocity. For robotic applications, low endeffector velocities inherently lower its kinetic energy and potentially diminish the ability of the endeffector to propel the metamaterial using inertial dynamics. Currently, the endeffector cycle frequency matches the actuated input frequency due to similar sampling of the target and generated trajectory to allow usage of the l^2-norm. Better objectives where this one-to-one precision point matching is not as strict in time could combine the best of both worlds regarding large design space and prescribing a well-known velocity where needed. Advancing any path-based objective function for use in robotic applications and using global objectives could be beneficial. Instead of prescribing the path that an end effector should follow for a walking gait, we may prescribe the overall motions of the robotic prototype. Specific amplitude and frequency combinations will cause the body to obtain a specific velocity in a specific direction, independent of any walking gait, allowing the metamaterial to figure out any geometrical structure that is optimal to obtain this velocity.

Outlook

Research into path-generating dynamic mechanical materials is making its first steps with this work. By exploring how well inverse design frameworks for metamaterials can generate trajectories, the forefront of a high-potential research area is here. Reflecting on Figure 1 where the qualities of a soft body give rise to different dynamical responses, the problem about multiple trajectories with a single mechanical metamaterial still stands. The current work explored multiobjective functions to search for a mechanical metamaterial with a reprogrammable dynamical response. This design space, where the endeffector makes two completely different trajectories, proved extremely difficult to navigate. The current framework supports this multiobjective approach, but the result can benefit from improvement.

We subject a 13×9 units mechanical metamaterial to two different individual sinusoidal inputs (14 and 18[Hz], with the same amplitude of 2[mm]) where the objective is to obtain a clockwise and counterclockwise elliptical endeffector trajectory, which means two individual dynamic responses coming from the same metamaterial. Theoretically, this led to a design capable of doing so, though experimentally, mediocre results were obtained (see SI section 7). Figure 10 shows the amplitude-frequency design space with two optimized trajectories and many neighboring points. One can easily see the evolution of size and direction (indicated by the green and yellow arrows), providing insight into this dynamic problem. We place a large emphasis on frequency, as it proves to be an important cause of multi-directionality. Improvements in

the tuning of mechanical parameters, improving the stiffness models used in the simulation, or the improvement of the used damping model, such as block-to-block relative damping instead of dashpots connected to the world, could provide great advancements in the realm of multi-gait path generation with mechanical metamaterials.

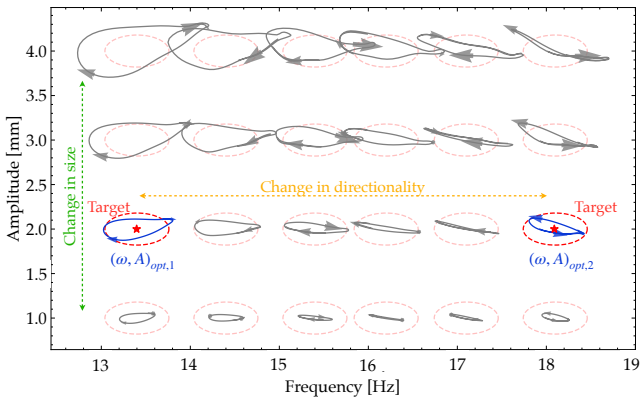

Fig. 10. Multiobjective trajectories: CW (left marked point) and CCW (right marked point) elliptical trajectories and the influence of different amplitude and frequency combinations.

Improving metamaterial robotics is the second contribution of this work, though it is not complete yet. Future work can revise the objective function, especially if robotics is the main application. For example, optimizing for propelling force or a global velocity can be more useful than optimizing for a certain endeffector path. This approach can lead to metamaterials propelling themselves more globally in previously unknown ways.

Different objectives create robotic metamaterials that exhibit multiple functionalities with a single geometry, incorporating the complicated control architecture within the metamaterial geometry itself. SI section 8 shows two scenarios of possible continuations into robotic metamaterials. On the one hand, changing the actuator input can change internal dynamics resulting in different endeffector trajectories and functionalities. On the other hand, external influences, such as bumping into an object, increase potential energy in the metamaterial. Since the internal dynamics closely relate to its internal energy, one can incorporate this change into the optimization to trigger the reprogrammability of the end effector trajectory.

In conclusion, whether robotic metamaterials can make use of this new framework or object-manipulating machines take advantage of path-generating mechanical metamaterials, the current research explored how mechanical metamaterials exploit internal dynamics for path generation and its applications within robotics. This field proves to have high potential, and future research into mechanical metamaterials can lead to advanced dynamic metamaterials and robotic systems.

1. R Rao, What are Robotic Assembly Lines? History, Components, Advantages, Limitations, Applications, and Future (2023).
2. J Gallardo-Alvarado, J Gallardo-Razo, Chapter 8 - mobility of mechanisms in *Mechanisms*, Emerging Methodologies and Applications in Modelling, Identification and Control, eds. J Gallardo-Alvarado, J Gallardo-Razo. (Academic Press), pp. 135–159 (2022).
3. X Zhang, B Zhu, *Introduction to Compliant Mechanisms and Design Methods*. (Springer Singapore, Singapore), pp. 1–24 (2018).
4. C Swan, S Rahmatalla, Topological design and control of Path-Following compliant mechanisms. *10th AIAA/ISSMO Multidiscip. Analysis Optim. Conf.* (2004).
5. CC Swan, SF Rahmatalla, Design and Control of Path-Following Compliant Mechanisms. *ASME* pp. 1173–1181 (2004).
6. A Saxena, Synthesis of Compliant Mechanisms for Path Generation using Genetic Algorithm. *J. Mech. Des.* **127**, 745–752 (2004).
7. P Jiao, J Mueller, JR Raney, XR Zheng, AH Alavi, Mechanical metamaterials and beyond. *Nat. Commun.* **14**, 6004 (2023).
8. J Wittenburg, *Degree of Freedom of a Mechanism*. (Springer Berlin Heidelberg, Berlin, Heidelberg), pp. 137–157 (2016).
9. B He, S Wang, Y Liu, Underactuated robotics: A review. *Int. J. Adv. Robotic Syst.* **16**, 172988141986216 (2019).
10. K Lochan, B Roy, B Subudhi, A review on two-link flexible manipulators. *Annu. Rev. Control.* **42**, 346–367 (2016).
11. A Ion, et al., Understanding metamaterial mechanisms. *ACM* (2019).
12. K Wu, O Sigmund, J Du, Design of metamaterial mechanisms using robust topology optimization and variable linking scheme. *Struct. Multidiscip. Optim.* **63**, 1975–1988 (2021).
13. G Bordiga, et al., Automated discovery of reprogrammable nonlinear dynamic metamaterials. *Nat. Mater.* (2024).
14. L Jin, et al., Guided transition waves in multistable mechanical metamaterials. *Proc. Natl. Acad. Sci.* **117**, 2319–2325 (2020).
15. AK Rai, A Saxena, ND Mankame, Unified Synthesis of Compact Planar Path-Generating Linkages With Rigid and Deformable Members. *ASME* pp. 223–232 (2009).
16. SS Schoenholz, ED Cubuk, Jax, m.d.: A framework for differentiable physics (2020).
17. DL Applegate, et al., *A Practical Guide to Discrete Optimization*. (University of Waterloo), (2014).
18. I Wolfram Research, l^2 norm from wolfram mathworld (2024).
19. S G. Johnson, GitHub - stevengj/nlopt: library for nonlinear optimization, wrapping many algorithms for global and local, constrained or unconstrained, optimization (2007).
20. UltiMaker, UltiMaker PLA for S series: Versatile, colorful, easy to 3D print (2024).
21. UltiMaker, S series TPU 95A - UltiMaker (2024).
22. UltiMaker, Ultimaker 3 Support community (2024).
23. Xeryon, Micro Linear Actuators - with Sub-Micron Precision (2024).

2 Literature Review

In this section, we introduce the research topic, explore the existing state-of-the-art, highlight the knowledge gap, and guide interest toward solving the unexplored knowledge gap.

"Exploring *Mechanical Metamaterials for Path Generation*: A Literature Review

Tom Vreugdenhil[*,**]

[*] *Delft University of Technology, MSc High Tech Engineering, Department of Precision and Microsystems Engineering, The Netherlands. In collaboration with Harvard John A. Paulson School Of Applied Sciences And Engineering, Harvard University, Cambridge, USA.*
[**] *T.E.vreugdenhil@student.tudelft.nl*

Compiled November 11, 2024

Mechanical metamaterials exhibit intriguing nonlinear collective dynamics under simple actuation, offering the potential for diverse displacementfields using a single physical mechanism. In the context of path generating robotics, where multiple actuators often rely on intensive control systems for precise manipulation, there arises a possibility to simplify these systems using mechanical metamaterials. This review considers the potential transition from intensively controlled robotics to metamaterial mechanisms, exploring how the unique properties of mechanical metamaterials might provide an alternative paradigm for achieving closed curve path generation with reduced reliance on external control. By seamlessly integrating this into the metamaterial topology, the study aims to transfer the burden of control complexity to the metamaterial itself. This literature review explores these principles and their application to achieve path generation through straightforward actuation. The review not only delves into the properties of such metamaterials but also discusses their broader significance in advancing the field and opening up new possibilities for path generating mechanisms.

1. INTRODUCTION

Within the realm of todays robotic industry many advancements have been made to create machines that can perform complex non-monotonic tasks at high speed to conduct as many tasks as possible in a small time-frame. Existing of mechanical linkages and joints which are precision-made to fit together if assembled correctly, these machines require many skills to build, calibrate and maintain to keep functioning in the long run. Especially in environments with food-safe conditions or medical areas, machine maintenance comes with issues regarding contamination and outgassing. High speed operation requires high speed actuators, one for each degree of freedom which can be many. Energy usage for the said actuators is therefore a problem of much concern, as prices are skyrocketing. To extend the energy usage, each actuator used comes with a control system, something that coordinates every movement as calculated by some processing unit. Often times, especially with machines operating near their resonance frequency, hard work is needed to ensure a proper control loop over an actuator to meet performance criteria as vibrations are a machines worst enemy.

The earlier reasoning not limited to noisy, big, and clunky robotic machines only but also applies to small-scale robotics. For example insect-scale robotics where downscaling effects obstruct the use of traditional linkages and joints. HAMR, a Crawling Microbot (Baisch (2011)) uses six legs to propel itself, requiring at least twelve actuators to perform a sweeping and lifting motion. This many actuators, control logic and internal energy supply make it difficult to obtain energy efficiency for long term usage.

Considering that these robotic mechanisms require actuation input to function, one can prescribe a precise path or cycle this input needs to possess. Generating such a path, especially in more than one dimension, can be achieved by using an equal amount of actuators as the required dimension with complex control software. Instead, path generation mechanisms can perform repetitive motion precisely driven by a single actuator, in which motion of the actuated part is embedded in mechanism components (Cheng, Song, Lu, Chew, and Liu (2022)). Designing a mechanism, such that a point on it traces a prescribed path when the mechanism is actuated is known as path generation and is already widely done using traditional rigid-body mechanisms, but are limited by creating one path only (Mankame and Ananthasuresh (2007)). Herein mechanism synthesis is performed, attempting to design the simplest mechanism that meets the requirements (Rai, Saxena, and Mankame (2010)). Compliant mechanisms effectively use their elastic deformation to transmit force and motion, such mechanisms derive their mobility from their embedded flexibility unlike conventional rigid-body mechanisms which use kinematic joints such as hinges for the same purpose (Mankame and Ananthasuresh (2007)). As no joints are present in compliant mechanisms, they can be produced in a large length scale, ranging from micrometers to meters. This makes compliant mechanisms ideal for small robotic insects to counteract downscaling effects. When compliant mechanisms are scaled down significantly, they transform into small unit cells that can be systematically arranged, or tessellated, forming an ensemble of miniature compliant mechanisms. The collective behavior of these units exhibits intriguing characteristics,

resembling a functional piece of material. In the spectrum from natural materials that possess intrinsic mechanical properties to large-scale structures which are characterized by design-specific structural properties, one can find a middle ground called metamaterials (Zadpoor (2016)). The tessellated internal structures, not the production material, define the mechanical properties of these structures. Specifically, mechanical metamaterials are engineered to exhibit superior mechanical features, such as ultrahigh stiffness and a remarkable strength-to-weight ratio, provided this information is embedded in the metamaterial structure. This makes them ideal as actuators to perform complex tasks using less energy compared with conventional approaches (Rafsanjani, Bertoldi, and Studart (2019)). Clearly path generation and metamaterials are widely researched, but not combined. This combination is exactly where passive materialistic intelligence could be created with great benefits.

In this literature review both fields are explored and the previously mentioned passive materialistic intelligence is sought as the gap between the two areas of interest in order to connect path generation and mechanical metamaterials for widespread functionalities. For this, the research question is formulated as: '*How can mechanical metamaterials generate* repeated *closed end-effector paths with a single input* for actuation of small-scale robotics'. With less emphasis on 'repeated' and 'actuation of small-scale robotics' as these are application related and limit the literature search space. The review is split into the two main areas of interest: 'path generation' and 'mechanical metamaterials'. Each domain is examined individually to acquire in-depth insights, contributing to the understanding of their possible interconnection. Their combination is thought of to be crucial in the future actuation of small-scale robotic mechanisms.

2. METHODOLOGY

In order to get a better understanding of how the rather soft mechanical metamaterials can fulfill path generating tasks in the realm of rigid-body robotics we perform a quantitative literature analysis on scientific papers published by well-known academic organizations like *The American Society of Mechanical Engineers* (ASME), *IEEE*, *ScienceDirect*, *SpringerNature* and *Association for Computing Machinery* (ACM) to name a few. Altogether, these sources create a trustworthy foundation for information retrieval which allows further analysis to be credible and valid. Extensive exploration is done to search, filter, categorize, review, summarize and report the relevant findings and to refrain from unnecessary repeating studies.

Repetition while comparing new sources is something of great value and should not be blindly discarded as this brings new insights and another authors view, Zadpoor (2016) and Pathak, Singh, Sharma, Kumar, and Chakraborty (2023) among others. Path generation and mechanism synthesis have been widely investigated and light is shed on kinematic equations, objective functions and constraints while being limited to mostly four-bar mechanisms. This review aims to go beyond traditional mechanisms and push towards synthesizing any path generating mechanism with a focus on including compliant mechanisms and mechanical metamaterials specifically to provide a novel bridge which, to the best of current knowledge, has not been previously implemented.

A. Search methods and selection

This literature review contains English-written frequently often cited, research, comparison, conference and review papers spanning from the early 1800's to present day while not being restricted to a specific period given that this is a thorough review, and not, for instance, an analysis focused on trends. To remain focused without overextending several keywords are developed, some examples include 'mechanism synthesis', 'compliant mechanisms', 'path generation', 'metamaterials', 'underactuation', 'shape features' and 'objective functions'. These are based on the growing collection of literature and scope of potential follow-up research. Next to keywords in a search engine, many review papers contain tremendous amounts of critical views on subexisting literature indicating their value. Often reviewing literature provides closely related new work with different keywords making it harder to find using the desired search terms. To extend the solutions to overcome difficulty, clever search engines are used such as Research Rabbit where artificial intelligence is applied to find trends in the collected literature and recommend closely related papers by different authors (*Research Rabbit* (2024)). It does so by providing network-like overviews with strings between cited or referenced work and indicating the existing library with green nodes and related work with blue nodes (Figure 1).

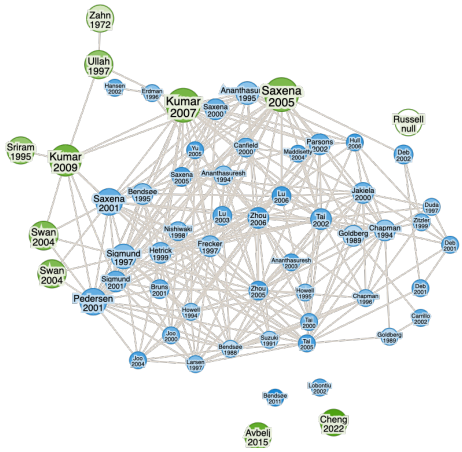

Fig. 1. Research Rabbit network

After screening and validating sufficient correlation between the found literature and area of interest the papers are read in its entirety. Mendeley, the online scientific standard for reading, annotating, filtering and working with sources provides a workspace to organize the collection (*Mendeley - Reference Management Software* (2024)).

B. Postprocessing the selected literature

Employing Mendeley is done by annotating while reading an article. Within notebooks the annotated parts are saved and collected per topic. After citing an interesting portion of the paper a critical comment or underlying explanation is added for later re-reading. Furthermore personal notes are taken with each scientific article that is read. Starting with summarizing the overall purpose of the article and providing criticism about the possible relevance in the work presented here. Next to this the most important takes are written down and potential expectations are made whether this is useful content for utilizing later on. At last the important sections are sorted per subject and diverse perspectives by the corresponding authors are challenged against each other to obtain a personal interpretation.

It has to be noted that this literature review is conducted in the short period of three months, without additional reviewers

to cooperate with. However the significant influence of discussions with fellow students, with the same background and not, cannot be left out as it frequently shed a new light on the discussed topics for a better understanding. Furthermore it is stated that not all literature is explored in-depth, much of the general information which is assumed to be common knowledge among engineering students is left out to concentrate more on identifying a gap between path generation and metamaterials and how to bridge this gap for a potential follow-up research project.

Concluding, this review should be seen as repeating pattern of broadening the researched topic, filtering, sorting and narrowing down to the most important highlights. Thereafter the process repeats itself with the goal of deepening the research without tunneling to one specific subject only and providing a strategical in-depth review of mechanical metamaterials, path generation and their possible combination.

3. FINDINGS

In this section, we delve into the key findings emerging from a quantitative literature review on the two main subjects which are *mechanical metamaterials* and *path generation*. As discussed in the methodology, this literature review aims to explore the individual realms, but more importantly explores the intersection between the two, uncovering insights and gaps in the current scientific knowledge. The purpose of this section is to present and briefly analyze the main findings extracted out of the literature, shining light on critical aspects of mechanical metamaterial behavior and its potential employment in path generation. Navigating through the intricate dynamics of coupled metamaterial cells, the design princples are explored which shape their behavior while discovering the unknown territories in their application for path generation. These findings do not only contribute to the readers understanding of metamaterial dynamics but also illuminate potential bridges to innovative use in path generating mechanisms.The findings will be presented in seven sections: collective dynamics of mechanical metamaterials (A), shaping the properties of mechanical metamaterials (B), practical implementations (C), rotating quads as structural modules (D), path generation in rigid mechanisms (E), shifting to compliant path generation (F) and categorizing shape features (G). Each individual section presents aspects of the literature and offer insights into the know-how of each subject. Readers are invited to reflect on these findings, identifying areas or research gaps for further investigation and possible novel new applications. The insights gained from this review are crucial in addressing the overarching question: '*Can mechanical metamaterials provide path generating capabilities?*'.

A. Collective dynamics of mechanical metamaterials

Harmonic mass-spring-damper systems are well understood and their dynamics can be interpret without much effort. When looking at metamaterials, especially if we consider metamaterials to consist out of many individual cells bundled together, the dynamics become exponentially more complex. An interesting take on active metamaterials, or as the authors call them 'active solids' by Baconnier et al. (2022), is by considering different states of bundled behavior. Their model showcases collective actuation resulting from the interplay between activity and elasticity since each unit is capable of performing work (polar, or dipolar, active forces around $\hat{n}$ (Figure 2)). The units in a collective solid are therefore seen to be an actuator once they interact as a collective. Nevertheless, *Baconnier et al.* shows interest in elastic solids with respect to active solids and explores the emergence of collective dynamics in elastic lattices connected at their corners which can be seen as closer investigation on passive structures such as metamaterials (Figure 2). Since each unit is

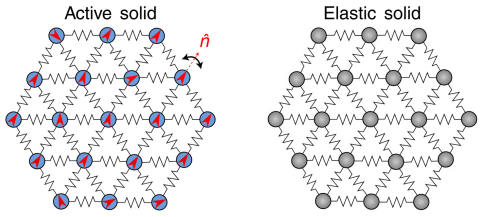

Fig. 2. Active and elastic solid, adapted from Baconnier et al. (2022)

interconnected to its neighbours some form of collectivity arises. Units can vibrate individually while barely disturbing surrounding units whereas the next boundary of units are not influenced at all. On the contrary, the whole bundle of units vibrate together in certain eigenmodes. These two zones can transform into one another depending on elasto-active feedback between multiple units, the larger it is the more likely it is to behave as a collective. There exists a threshold π_{FD} where the solid is frozen, further along is a second threshold π_{CA} where collective action starts and synchronous oscillations are observed in (Figure 3). In between, regions of frozen and collective motion exist indicating hard to predict activity. This region raises challenges in predicting the individual and global dynamics which calls for simulation and optimization were this to be transformed into a real world application. Observing the properties of individual

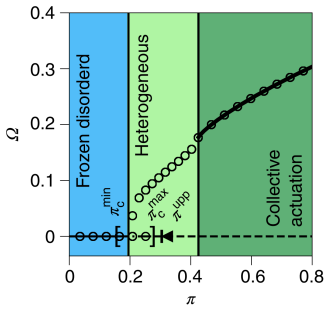

Fig. 3. Single unit vibrating phase diagram, adapted from Baconnier et al. (2022)

and collective behavior brings rise to questions regarding practical application of similar metamaterial-like structures and the possibility of designing for desired behavior. Contributions have been made with optimization schemes to assign specific properties to the designed metamaterial structure, these include negative Poisson's ratio, negative compressibility, negative thermal expansion and vanishing shear modulus (Surjadi et al. (2019)).

B. Shaping the properties of mechanical metamaterials

Upon uniaxial stretching, conventional materials experience longitudinal extension along the stretch direction and lateral contraction perpendicular to the stretch direction. The Poisson's ratio of a material is defined as the negative ratio of lateral to longitudinal strains. In conventional bulk materials, Poisson's

ratio typically ranges from 0 to 0.5 and is a positive value (News and Lakes (1993)). Poisson's ratio is defined as $\nu = -\frac{\varepsilon_T}{\varepsilon_L}$, the negativity means they expand under tension and contract under compression (Figure 4). The negativity is therefore originating from equal sign strain values in horizontal and vertical direction, easily proven with the use of auxetics (Grima and Evans (2000)). Stepping up in functionality we find the intriguing pentamode

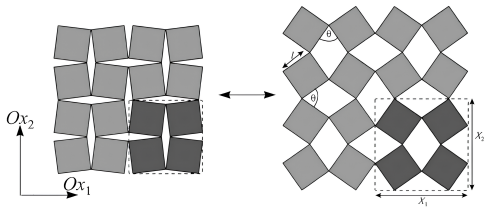

Fig. 4. Auxetic behavior in rotating squares, adapted from Grima and Evans (2000)

metamaterials, also known as metafluids. The bulk modulus in these metamaterials is extremely high with respect to the shear modulus, therefore the volume remains constant while deforming, but almost flow away while shearing (Figure 5). The combination of these arising properties mean it is difficult to compress but easy to deform in shear (Kadic, Bückmann, Stenger, Thiel, and Wegener (2012)). Furthermore metamaterials with negative stiffnesses deform while providing an additional deformation force and thereby assisting the total deformation. This could mean unstable deformation, so constraints or neighbouring sections of positive stiffness are required to keep chaos at bay. As a result, in multiple studies it is shown that materials with both positive and negative stiffness combinations exhibit remarkable properties, including exceptionally high damping coefficients (Lakes, Lee, and Bersie (2001)). Several materials displaying negative stiffness are linked to bi-stability (having two stable states) and snap-through behaviors, meaning a very binary or discontinuous switch in mechanical properties but well scale-able. A crucial application of materials with negative stiffness is the simultaneous availability of high damping and high stiffness. This combination looks promising in the applications for vibration isolation.

Another essential mechanical characteristic is ultra-lightweight, as ideal construction materials are anticipated to possess both ultra-stiffness and ultra low density according to Shaikeea, Cui, O'Masta, Zheng, and Deshpande (2022). Yet, as of this moment optimizing the stiffness and density of materials poses a significant challenge. Mechanical metamaterials provide a solution to this problem, allowing the design of material systems with tunable stiffness and density (Lin et al. (2018)). Researchers have also discovered that mechanical metamaterials may exhibit negative compressibility transitions, characterized by longitudinal deformation in response to an applied longitudinal force, which is unexpected and counter-intuitive (Nicolaou and Motter (2012) and Grima and Caruana-Gauci (2012)). Utilizing the intricate microstructures with interconnected elements capable of storing and releasing energy, mechanical metamaterials can show tunable properties, such as the earlier negative compressibility. These features enable them to dynamically respond and alter their shape across a wide range of scenarios in response to external influences.

The intricate microstructures embedded in mechanical metamaterials unlock a diverse array of mechanical properties,

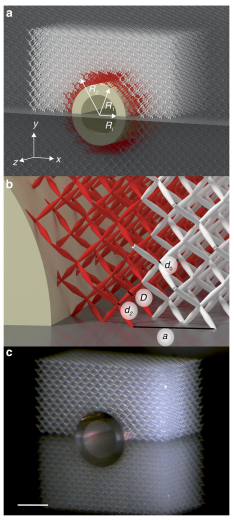

Fig. 5. Unfeelability cloak to elastically unfeel objects made with pentamode metamaterials, adapted from Bückmann, Thiel, Kadic, Schittny, and Wegener (2014)

paving the way for versatile shape changes and adaptive load-bearing responses. These characteristics are highly sought after for the envisaged advancements in soft, smart materials. The ability of these materials to dynamically alter their configuration and efficiently bear loads positions them as key players in the evolution of future engineering.

Moreover, such behaviors exhibited by mechanical metamaterials serve as pivotal ingredients in the synthesis of controllable combinations of static and dynamic responses within autonomous engineered materials. This not only underscores their potential in responding to environmental stimuli but also positions them as promising candidates for the creation of sophisticated materials that seamlessly integrate with various applications and contexts. In essence, the microstructural intricacies of mechanical metamaterials hold the promise of shaping the future landscape of material science and engineering.

Mechanical metamaterials exhibit complex collective dynamics, as evidenced by *Baconnier et al.*'s model. The interplay between individual cell-like dynamics results in emergent collective behaviors. The dynamical phase diagram introduces challenges in predicting these dynamics, emphasizing the need for advanced simulations. This complexity lays the groundwork for potential real-world applications. The ability to tailor mechanical metamaterial behavior for specific properties opens avenues for diverse applications. Optimization schemes successfully assign unique characteristics such as negative Poisson's ratio, negative compressibility, and vanishing shear modulus. These engineered properties defy conventional material behaviors, establishing metamaterials as versatile building blocks (Surjadi et al. (2019)). Mechanical metamaterials showcase unique properties, including negative Poisson's ratios and the intriguing behavior of pentamode metamaterials valuable in vibration isolation applications according to *Kadic et al.* and *Lakes*. The tunable properties of mechanical metamaterials address challenges in optimizing stiffness and density, presenting a solution for ideal construction materials. Counter-intuitive transitions, such as negative compressibility, highlight the unconventional nature of these materials (Shaikeea et al. (2022)). These characteristics are pivotal for advancements in soft, smart materials. There-

fore, microstructural complexities of mechanical metamaterials hold the promise of shaping the future of material science and engineering, offering a paradigm shift in controllable material responses.

C. Practical implementations of mechanical metamaterials

Mechanical metamaterials promise real-world breakthroughs beyond their theoretical properties as found in a lab example, therefore revolutionizing engineering in areas such as robotics and aerospace with their lightweight, ultra-stiff, and shape-changing capabilities.

New opportunities in the design of non-rigid mechanical metamaterials are upcoming with applications in for example shape morphing. To bring about significant shape changes in an object, it must possess a degree of softness, either in material properties like a low elastic modulus or geometric characteristics such as slenderness. Work into this field, combining soft matter physics, mechanics, applied mathematics, biology, and materials science, aims to utilize elastic instabilities for mechanical functionality, expanding our understanding of structural stability for form and function. Precise control of pixelated structures allows programmable deformation across multiple length scales, showcasing the ability to create intricate shapes, like a cube transforming into a smiling face under uni-axial compression (Coulais, Teomy, De Reus, Shokef, and Van Hecke (2016)). The intentional manipulation of geometry and elasticity to create adaptive, morphing structures heralds a new era of designer materials. An elegant demonstration involves controlling volumetric strain through the non-homogeneous pneumatic inflation and collapse of soft, elastic plates (Siéfert, Reyssat, Bico, and Roman (2019)). Shape-shifting materials require navigating the constraints of elasticity and employing non-linearity to generate functionality. The open question remains: how do we transform shape-shifting building blocks into programmable generic structures? Exactly that, applied in path generation, is a gap in the world of mechanical metamaterials that seems to remain a blank spot.

D. Rotating quads as structural modules

Auxetic behavior is a common viewpoint for the design with rotating squares. Research conducted into this elegantly structured metamaterial mechanism proved itself useful in creating negative Poisson ratio's (Figure 4). An idealized rotating structure contains rigid squares connected through simple hinges. When loaded, the squares will rotate at the vertices, either expanding or contracting depending on the loading type (Grima and Evans (2000)). The idea has been extensively applied using squares, rectangles, and triangles. *Grima et al.* applied the conservation of energy principle to simulate this behavior, demonstrating that the idealized system consistently retains its aspect ratio, resulting in constant Poisson's ratios of -1. The results of their experiments verify the promising nature of these systems, which may be engineered to exhibit a variable pore size and/or shape to achieve further functionalities. Variable pore size, or different rigid-body square shapes, could open the door towards strange and more difficult, even deformation-varying Poisson ratios. This opening would call for optimization procedures as their deformation quickly becomes too difficult for analytical analysis. Building on top of *Grima et al.*'s work, a set of rotating squares, individually connected at their corners, might be considered a building block if their rectangular-shape is to be differentiated from the usual, resulting in stretched or scaled polygons with four vertices paving the way into deformations that can be wildly different from simple extension or contraction, and maybe even with curved (open or closed) deformation building upon bi-stability or inertia of the rigid quads if dynamics were to be included. That is important, as all work into translating and rotating quads up until today is done in quasi-static environments. Higher speed motion accompanied with changing square geometries enrich the already known quasi-static results and could be of great value in future researches.

E. Path generation in rigid mechanisms

Traversing a predefined trajectory with the end-effector (usually on the coupler link) of a traditional rigid-link mechanism is known as path generation, and optimizing each link to obtain the best performing mechanism is called mechanism synthesis. These techniques are old theory nowadays as one of the, if not the, first research into this subject is done by Kempe (1875). In this work, *Kempe* calculates the traversed motion of some link within his mechanism. It is stated that even multiple trajectories are possible, even double curved in multiple directions as long as the input is altered accordingly. Since this work came out in *1875* there is no optimization done, but *Kempe* strongly calls for '*mathematics artists to discover the simplest linkworks that will describe particular curves*'. Years later *Russell et al.* consider two-and-three-dimensional four-bar-linkages with simple revolute and spherical joints respectfully with the aim of generating motions. Interesting to denote is that their motions can become quite complex with different speeds due to the varying pivot position in their mechanism as the motion is induced (Russell and Sodhi (2001)). This offers a wild range of possible motions, however the practical application is difficult to achieve, also indicated by no physical proof in *Russell et al.*'s research. Furthermore, a growing number of works have employed evolutionary strategies to address challenges in mechanism synthesis (Cabrera, Simon, and Prado (2002), Cabrera, Nadal, Muñoz, and Simon (2007) and Shiakolas, Koladiya, and Kebrle (2002)). The simplicity in applying the algorithms and their ease of computation make them one of the better competitors. Solving dimensional mechanism synthesis problems therefore comes with better and better accuracy and results. Though different routes can be taken, such as Genetic Algorithms, Particle Swarm Optimization and Differential Evolution. Especially Differential Evolution, which was introduced by Storn and Price (1997), has been successfully applied in several other optimization problems. *Cabrera et al.* perform mechanism synthesis with this method and successfully calculate error functions and several examples to prove their algorithm is valid in four and six-bar mechanisms (Cabrera, Ortiz, Nadal, and Castillo (2011)). Within the algorithm, the desired curve is compared with the generated coupler curve and their constraints are enabled using penalty terms in the objective function. With respect to previous synthesis solutions, their MUMSA ((Malaga University Mechanism Synthesis Algorithm) improves previous comparative work. All above mentioned techniques have considerably many design variables and *Sardashti et al.* take the approach with a GSEF (Geometric Similarity Error Function). Its number of design variables is less and by applying an Innovative Adaptive Algorithm their work is fast, takes less CPU time and saves on computer memory (Sardashti, Daniali, and Varedi-Koulaei (2022)). The elimination of design variables includes the centroid position of the generated curve and its orientation to an origin, meaning the curve can be optimal but needs to be translated, scaled or rotated accordingly afterwards. Everything mentioned up to here considers mechanism synthesis in two dimensions, but it is certainly not limited to that.

Exact 3D path generation is a fundamental problem of designing a mechanism to make a point exactly move along a prescribed three dimensional path, driven by a single actuator. A mechanically beautiful approach is taken by *Cheng et al.* where Cam-Linkage mechanisms are employed to do exactly so. A three degrees of freedom (DOF) five-bar spatial linkage is modeled to exactly generate a prescribed 3D path. Then, the spatial linkage's DOFs are reduced from three to one by composing the linkage with two 3D cam-follower mechanisms. This ensures minimizing the weight while having smooth, collision-fee and singularity-free motion of a path with C^0 continuity (Chiandussi, Bugeda, and Oñate (2000)). In their three-dimensional cam-linkage mechanisms, two crucial components are spatial linkages and 3D cams. Spatial linkages play a vital role as primary mechanisms for 3D path generation, with the choice typically being between four-bar and five-bar linkages. They opt for a five-bar spatial linkage and clarify why a four-bar spatial linkage falls short of meeting their objectives in their supplementary material.

For precise 3D path generation, their chosen five-bar spatial linkage should possess three degrees of freedom (three DOFs). Instead of relying on three independent actuators to control these DOFs, they propose the use of 3D cams (Cheng, Sun, Song, and Liu (2021))). This approach aims to govern the motion of the linkage and, in turn, reduce the overall DOFs of the entire mechanism from three to one, enabling it to be operated by a single actuator (Figure 6). It is worth noting that planar cams are unsuitable for this task, as they can only transfer one-DOF motion to another one-DOF motion. With this work *Cheng et al.*

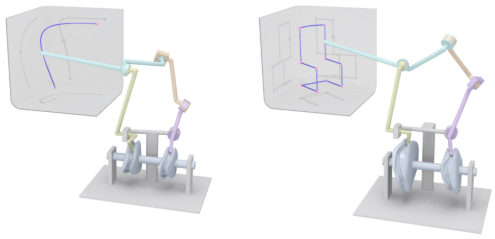

Fig. 6. Several 3D cam mechanisms, adapted from Cheng et al. (2022)

demonstrate that their mechanism is capable of exactly following any 3D path with a precision of less than a floating point (Cheng et al. (2022)) which is impressive.

Nearly all exact mechanism problems, especially the ones mentioned up to now, involve the use of rigid-link mechanisms, which are robust systems following a defined path. However, this inherent rigidity imposes limitations, as dedicating one mechanism to a specific curve proves inefficient when targeting diverse functionalities. Moreover, wear and play affect each mechanism, leading to a loss of precision as they degrade over time. This situation prompts the need for enhancements.

F. Shifting to compliant path generation

One of the first methods for optimal design of compliant mechanisms is presented by *Sigmund et al.*. The method is based on continuum-type topology optimization techniques and finds the optimal compliant mechanism topology within a given design domain and a given position and direction of input and output forces. By constraining the allowed displacement at the input port, it is possible to control the maximum stress level in the compliant mechanism (Sigmund (1997)). This is however an apriori guess, which is not included in the optimization process and only validated afterwards. *Sigmund et al.* strongly advice next steps to be taken in the realm of stress constraints, so they acknowledge their design flaw. Several examples with handgrippers, crunching mechanisms and displacement inverters prove the workings of the formulated theory. The first extension needed is to implement direct stress constraints in the formulation, but will slow down computational speed, though it will also result in different and improved optimum mechanism topologies. Further research into compliant mechanisms with real functions, such as path generation, is done by Kota, Hetrick, Li, and Saggere (1999). Using an energy based approach for comparison between input and output, they neglect mechanism dynamics and damping losses and focus on energy storing elastic members. Similar to Saxena and Ananthasuresh (2001a) and Saxena (2005) the design space is discretized into horizontal, vertical and diagonal elements. Therefore, and while acknowledging that this is published in 1999, the generated mechanisms are very similar to rigid-link mechanisms with small bending elements at the endpoints of an element. Interesting is that the first four natural frequencies of the force amplifier example are calculated, hinting towards investigating its dynamics. The result of this analysis shows the second natural frequency to be orders of magnitudes higher, indicating a severely robust system. Clearly shown to be pioneers in this field *Sigmund et al.* and *Kota et al.* show their willingness to come up with improvements, however how much of an improvement can it really get to?

While rigid-body mechanisms can be optimal in innumerable macroscopic mechanical systems, they are generally less suited for micro-scale applications due to the fundamental difficulty of fabricating reliable hinged-joints on such small scales. One potential answer to this problem is to employ compliant mechanisms (Swan and Rahmatalla (2004)). The elastic deformation in compliant mechanisms may either concentrate in flexible hinge regions or distribute more uniformly throughout the mechanism. Typically, efforts are made to redesign the hinged joints of rigid-body mechanisms as flexible hinges (Figure 7), aiming to achieve performance roughly comparable to that of the rigid-body mechanism. However, compliant mechanism designs incorporating distributed elastic deformation may offer increased design flexibility and durability. In *Swan et al.*'s time,

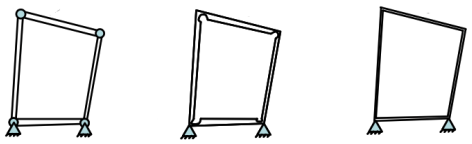

Fig. 7. Left: rigid-body mechanism, middle: partially (lumped) compliant mechanism, right: fully compliant mechanism, adapted from: Swan and Rahmatalla (2004)

exploration of continuum topology optimization methods for achieving path-following compliant mechanisms was still in its early stages, with only a limited number of papers published on this topic (W Pedersen, Buhl, and Sigmund (2001) and Saxena and Ananthasuresh (2001b)). *Swan et al.* propose the use of two sets of springs to achieve path-following performance. These springs regulate discontinuities rather than relying on rigid connections, presenting both very stiff and very small resistances. The approach involves initially applying the stiff springs to achieve a stiff yet optimized design, followed by substituting

the softer springs to assess the actual deformation performance. When applied to an inverter path-following example, *Swan et al.* demonstrate the successful synthesis of a fully compliant design that generates an approximate straight line at the output port. It is important to note that this framework primarily solves for the required input force, and the author suggests further exploration on the control side.

Rai et al. propose a procedure for synthesizing path-generating planar linkages whether they are rigid-body, partially compliant or fully compliant. Here partially compliant is defined as containing some compliance and fully compliant as lumped compliant. The synthesis task is formulated as a constrained optimization problem and is addressed using a hybrid, elite-preserving genetic algorithm. To illustrate the synthesis capability of the procedure, three examples of compact mechanisms that trace different non-smooth paths in response to a single, monotonic, and bounded force input are employed (Rai et al. (2010)). One can observe that in all three examples, partially compliant mechanism designs offer better conformance with design intent than either rigid body or fully compliant mechanisms. This is contrary to what Swan and Rahmatalla (2004) tries to achieve, as fully compliant mechanisms easily cope with internal stresses with respect to partial compliant variants. *Rai et al.* claim that the introduction of internal DOFs into simple linkages is yet another way to improve their geometric capability without sacrificing practical utility. This could mean that utilizing fully flexible, or metamaterial-like, members which contain many internal DOFs could be a viewpoint for improvement. The authors do not further touch upon this subject. Robustness is briefly touched upon as the input port must be moved non-monotonically, meaning non-linear difficult input control, along a predefined line or the mechanism will produce a severely different path. However, robustness in terms of counteracting forces at the end-effector is taken into account by having a resistance force during the optimization cycles. Their examples show that partially compliant mechanisms exhibit greater geometric capability than either rigid body or fully compliant mechanisms. This is straightforward knowledge, as a rotary input is required in traditional four-bar linkages for creating a closed end-effector curve. Material failure and fatigue are deliberately not included in their work.

Saxena continues to work on the subject as done with fellow researchers in Rai et al. (2010). In this work not only is the linkage length determined for a compliant path following mechanism, but also the topology of each complaint member. To model the size, cross sections of frame elements they may be additionally treated as design variables meaning a more complex problem to solve. Geometrically nonlinear analysis is performed with the optimization power of genetic algorithms. *Saxena* therefore included a very binary approach in the objective function, as the design space is discretized and a member is present or not. The result is a fairly box looking structure with horizontal, vertical and diagonal members. The more difficult objective function, and direct optimization of shape, size and position is well defended, since it allows to solve large displacement nonlinear compliant mechanisms in their binary form, it circumvents problems with non convergence or buckling and the end result can be interpreted as is, no further post processing is required making it a complete total package.

An open loop compliant mechanism consisting of two elastic links actuated through piezoelectric actuators has been analyzed by Banerjee, Bhattacharya, and Mallik (2009). The links may be joined through rigid or elastic hinge connection. Meaning a different approach to path generation, with only two (actuated) members, which should be able to span the whole two dimensional plane. *Banerjee et al.* denote the importance of analysis a bending beam due to external moments as this is the base of their mechanism. Ultimately they investigate how two connected beams interact and analytically derive the end-effector displacement. Inverse kinematics are calculated to obtain two parameters which need optimization, namely the input moments.

G. Shape features

Path following compliant mechanisms are nowhere without the ability to differentiate between shapes for obtaining a score-value to assign to a generated path with respect to a desired path. This means encoding a shape into numbers with which we can start scoring. Traditionally, the reference path is point-wise compared with the generated path in terms of equally sampling along the contour or perimeter, also known as the brute approach. Brute in the sense of requiring many sampled points along the curve which are compared individually per X and Y-coordinate. A different and more often researched way of comparing shapes is with the use of turning functions.

Turning functions are functions that capture the overall rotation of a given curve (continuous) or polygon (piece-wise linear) and originates from Arkin (1989). The turning function is one dimensional and is used as a description for representation of two dimensional shapes. *Volotão et al.* claim that any finite polygon that can be represented in a euclidean plane can be transformed into a turning function. This comprises of the relation between tangent angle and arc length and starts from some point on the curve and follows the curve counter clockwise (Cosgriff (1960)). The turning function can compare the desired and generated path and it is not influenced by size, location and orientation of the mechanism, making it ideal for true shape comparison (Nadal, Cabrera, Bataller, Castillo, and Ortiz (2015)). The authors

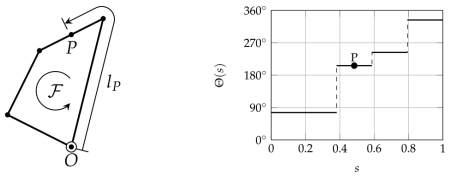

Fig. 8. Polygonal shape $\mathcal{F}$ with its turning function $\Theta(s)$, adapted from Volotão, Santos, Erthal, and Dutra (2010).

declare downsides too, a turning function is sensitive to noise, it has a computational cost associated with matching and it may cause errors when the border of the shape is slightly changed (Zhang and Lu (2004)). In addition, the arc length grows locally with noise resulting in the whole perimeter increase. However, the main advantage is that the comparison between the desired and generated path does not vary with rotation and translation of the mechanism. Therefore the design variable vector does not include the parameters which define fixed link position and rotation, diminishing searching space (Nadal et al. (2015)). This results in a synthesized mechanism, that is capable of creating the desired curve, but the position and orientation could be far off.

Torres-Moreno et al. propose a new method to represent paths: normalized shape-descriptor vectors (NSDVs), which are similar to turning functions but simpler to define. Instead of comparing coordinates, this approach focuses on measuring the similarity

of the desired and the obtained curve by studying their intrinsic properties such as radius of curvature or arc length. This increases the flexibility at search and involves less optimization variables to handle because the assessment is not biased by the necessity of matching coordinates, but it evaluates the underlying differences in shape (Torres-Moreno, Cruz, Álvarez, Redondo, and Giménez-Fernandez (2022)). As it occurs with turning functions or the method proposed, shape codification strategies achieve flexibility by becoming invariant to changes in scale, rotation, and translation of the curves. Thus, it is ultimately necessary to transform any configuration found to make the output of the corresponding mechanism not only equivalent to the target in shape but also in size and orientation. Otherwise, the resulting mechanism might replicate the target shape, but it could not work in the same context. The author is clear about the downsides, NSDVs are limited to simple polygons (either concave or convex), without self-intersections. They do not allow to compare polygons with a different number of vertices either (as the resulting vectors have a different number of dimensions). This makes NSDVs a relatively new competitor in the field of path generation. Especially when compared with the Fourier methods described next.

Fourier descriptors, initially proposed by Cosgriff (1960) as a set of numerical representations encapsulating the form of a closed curve, consist of amplitude and phase coefficients derived from a Fourier expansion of the turning functions associated with the curve. However, a more comprehensive explanation of the operational principles can be found in the work of Zahn and Roskies (1972). The process involves selecting a starting point on the boundary, defining a function that measures the angular direction of the curve relative to arc length, normalizing this periodic function, and expanding it into a Fourier series. The coefficients of a truncated expansion serve as shape features termed Fourier descriptors. Since the mathematical details are well explained by *Zahn et al.*, they are not extensively covered here. Fourier Descriptors capture shape; however, if the shape undergoes rotation, translation, or scaling concerning the desired form, additional information needs to be incorporated into the objective function. Alternatively, separate optimizations can address these transformations. *Zahn et al.* merely introduce the topic of Fourier Descriptors, later this is put into use for mechanism synthesis for the first time by Ullah and Kota (1997). They denote that the function used is very sensitive to double looped curves in comparison to single loop curves. However, with respect to corresponding brute force methods, the nonlinear and multi-modal Fourier function is not overly complex (Ullah and Kota (1997)). Furthermore they enrich the background of Fourier descriptors, indicating that the method only returns relative link dimensions in a four-bar linkage without any specification to position, rotation and scale once again restating the invariances.

In the realm of image processing this method can really show its capabilities as the invariances are used as an advantage. They are deployed in image processing for x-ray scans to recognize vertebral images (Lee, Antani, and Long (2003)). They calculate a similarity value (percentage) using the amplitude component of the Fourier descriptors, do this effectively and prove this with examples to be feasible too. Returning to mechanism synthesis, *Mankame et al.* continue the work of *Ullah et al.* with contact aided synthesis to achieve non-smooth paths while maintaining a single monotonically input force. They improve the objective function by incorporating a perimeter and orientation value to combat the invariances of the Fourier approach. Furthermore they experiment with including the input force as design variable as to account for resistance forces. They recall that this is not straightforward as it leads to cumbersome expressions in sensitivities (Mankame and Ananthasuresh (2007)). Their application for contact-aided compliant mechanisms it successful, but recommend to do further explorations on the input force as design variable.

A wild step away from real mechanism synthesis is done by *Khan et al.* since they employ a trained artificial intelligence (AI) model to create possible four bar linkage designs with only the prescribed input path (in Fourier description) as total input to the AI model. This is a direction that seems very promising in terms of creative alternative designs, especially if this power is utilized for something more complex than a four bar linkage. Although four-bar coupler curves have wide-ranging shapes, it should be noted that the method is limited to simple, closed curves; open curves (such as those produced by double-rocker mechanisms) and curves with crunodes are excluded (Khan, Ullah, and Al-Grafi (2015)).

Reverting to optimization in mechanism synthesis without the use of AI, but nonetheless in a modern day work, *Guo et al.* reviews the Fourier Descriptor method very well. By laying this method next to the brute force approach, among others, a strong recommendation is the most important lesson learnt. Their work proves that the combination of different trajectory approaches leads to a better synthesis performance, which is believed to provide new ideas for developing more efficient mechanism design methods (Guo, Zhang, Wu, and Yao (2023)). Meaning that from 2023 and onwards they foresee different path generating approaches to enter the realm of mechanism design.

Other shape comparing methods have, in the meantime, been addressed, and the following contains great potential to enter as a newcomer in path generation. The metric for Polygon and Line Segment comparison (PoLiS) is introduced by *Avbelj et al.* The PoLiS metric is a positive-definite and symmetric function that satisfies a triangle inequality. It accounts for shape and accuracy differences between the polygons, is straightforward to apply, and requires no thresholds (Avbelj, Muller, and Bamler (2015)). The metric compares polygons, not only point sets, with different number of vertices and is insensitive to a mismatch in data points within the polygon. PoLiS is not invariant to translation, rotation or scaling, as the authors developed it to recognize building footprints where only shape similarity is not enough. They claim the PoLiS metric to be straightforward to implement and responding approximately linearly to changes in the translation, the rotation, and the scale, meaning that it is suitable for optimization. No introduction to mechanism synthesis is done, as far as current knowledge goes, it is only briefly touched upon by Torres-Moreno et al. (2022), but it holds great potential to do so.

More than plenty types of shape distinguishing are available, which could be suitable candidates for path generating mechanism synthesis. Each method calculates a similarity value, or the opposite an error value. For optimization this error function should be coupled to the design parameters of the building blocks of a mechanism basis, such as a four-bar linkage or in the more interesting case; mechanical metamaterials to obtain a solvable objective function.

4. DISCUSSION

Following up, one should be critical to raise questions about these findings and compare the different researches to assign validity. Here the heterogenous zone in metamaterial dynamics is

investigated, designed properties are related to these dynamics, a different view on ultra-high or ultra-low properties is given, inertia, strain and vibrations are discussed in practical applications. Then continuing with critical views on rigid-body path generating mechanism in terms of control complexity and material wear, following up with the shift to compliant path generating mechanisms where microstructures and material defects, path following performance, more internal DOFs, resistance forces and fatigue are adressed. And eventually differences, up-and downsides, the use of AI and other shape comparing properties are presented. At last the bridge between mechanical metamaterials and path generation is highlighted, which is considered of utmost importance as a result of this literature review.

Considering the grey zone, the mixture of frozen and collective dynamics, in Baconnier et al. (2022) it is interesting to think about the potential upsides of this difficult to predict phenomenon, or about the downsides which need to be diminished . Especially if we consider multiple collective vibration modes, does the grey zone reappear in the shift towards the next and can it give (visual) information on the type of transition. Areas where frozen states exist next to oscillating ones, there is an interplay at their boundary. *Lakes et al.* claim that within metamaterials areas with a negative Poisson ratio can exist, but must be assisted by positive ones or another form of constraint to ensure stability. Combining this with the chaotic interplay in the mixture zone shows similarities if the grey zone is seen as a design intend to create this negative-positive Poisson combination. Perhaps dynamic structures which change in shape or size can give rise to new inventions for example expanding moving mechanisms where the movement can now be seen as intentional instead of the enemy. On the contrary, diminishing the undesired grey zone is the other way of thinking, does this change the transition towards collective behavior in a negative manner? That would mean it is different to move between vibration modes as their transition is not as fluid but very abrupt, or does not exist at all since it is harder to escape a mode.

The elasic model, as depicted in Figure 2 contains a well-ordered structure of units, with equal spacing everywhere. Interesting auxetic behavior with a similar equally spaced structure is reported by *Grima et al.*, but is limited in terms of practicality. The authors experiment with differently ordered structures, but only different Poisson ratio's are observed while the potential for more is there. Variable pore size for example, creating a non-equal spacing between units and a non-equal unit shape. This could lead to varying effects such as completely different Poisson ratio zones next to eachother, where local strain is highly important due to continuity between zones if it is not gradually changing. Another point of interest is the inclusion of dynamics, since up untill now all auxetic structures (and most similar metamaterials) operate quasi-static. In the case of unevenly spaced and shape varying squares (an adaption of Figure 2) inertia now regulates the deformations over time and introduces vibrations. Furthermore the intertia combined with elasticity can utilize storing energy in the connections for release in the reversing part of the input cycle (Tantanawat and Kota (2006)). Power usage can be lowered, especially in dynamic applications. This is an interesting field of research, especially if one tries to match this to the observed dynamics of Baconnier et al. (2022).

Interesting dynamics need an application, *Russell et al.* proposes a rigid-link mechanism with a moving pivot. Theoretically this is solid, but in practicality not so much which coincides with the absence of any experimental work. Adding a moving pivot increases the internal DOF meaning more complex end-effector motions, however this requires an additional actuator which comes with extra control complexity and energy usage. Or this pivot must be mechanically connected to take away the extra DOF, while keeping positional flexibility, with the downside of limiting the end-effector motion. Zooming out, is this even worth it? If additional actuators keep being added we end up with dynamics similar to an infinitely many linked pendulum which get increasingly difficult. This is not the right path to go, but a more novel approach would be to remove rigidity and introduce elastic structures. This could be a energy-efficient, high DOF and easy to fabricate alternative.

This shift towards elastic structures is well established in this literature review. *Swan et al.* describe the durability of fully distributed compliant mechanisms to be a key factor for choosing this approach. However this contains its difficulties in designing such a structure. Yes, if a four-bar linkage is replicated, then each member follows simple beam theory and for this we know analytical solutions. But once the mechanism gets more complex, beam theory is out in the wild. Keep in mind that material defects greatly influence deformation behavior, but that it is not all a negative thing. If the inner structure of this beam, similar to material microstructures, is designed with small compliant structures (metamaterials) using for example evolutionary techniques, then this beam can be designed to exhibit specific deformations thanks to many addtional DOFs (Rai et al. (2010)). In this way, distributed compliant mechanisms easily surpass the realm of four-bar linkages instead of being just comparable. Designing a flexible four-bar mechanism is holding back a design method with tremendous potential, as these traditional mechanisms rely on rotary input to create closed curve end-effector paths which cannot exist in compliant mechanisms as it violates elastic strain limits. Closed curves can be achieved using bi-stability, but that is very binary behavior and outside of the scope of this review.

Closing an end-effector path is easy without resistance forces, but if any application is desired then this force must be taken into account. The path can be showcased using a videorecoring with point tracking which requires no additional force, but more hands-on would be to include something to write on a sheet of paper. Any additional force, not considered in optimization, can completely change the mechanism behavior. *Mankame et al.* try to include the input force in the optimization and apply a resistance force, but leads to cumbersome expressions in sensitivities. Optimization is therefore increasingly difficult, the computational cost increases and stability near singular points of the solution is far from guaranteed.

Working with objective functions is essential in optimization and in path generation there are numerous ways to setup this function in terms of shape features. Turning functions have been discussed previously and work with integrating the function to obtain an area measure. Though a very easy computation, it can be argued that area alone is not enough. Take two shapes, a square ($1x1$cm) and a circle ($r = 0.56419$cm), in terms of area they have the same value so a turning function objective cannot distinguish between them. Potentially by also including the derivative of this turning function into the objective one can clearly distinguish the two, but this is not done in current literature. Also turning functions are known to be sensitive to noise on the perimeter and invariant to size, orientation and position, making them ideal for shape recognition but not for exact shape positioning (Volotão et al. (2010)). Fourier descriptors

add extra measures to turning functions in terms of expanding into a Fourier series and using individual coefficients as shape measures. The size of these terms and their position in the series already enables for more distinguishing between two shapes of equal area. On top of that this measure is truncated to only keep the most important features of a curve, usually 10 terms is enough to characterize a whole shape instead of many datapoints as done in turning functions, therefore computing should be more efficient. Then again, Fourier descriptors are invariant to size, orientation and position, however attempts exist to combat these. *Mankame et al.* incorporate total perimeter length and orientation to the objective function and this eliminates size and orientation. Overall position remains, but considering these attempts rely on four-bar mechanisms, they argue that simply replacing the total mechanism takes care of this last variance. On the contrary, in for example a metamaterial structure, where building space is very limited, this approach is generally not suitable making the Fourier approach an interesting competitor but not the best. An overview regarding shape feature highlights, downsides and ease of application is given in Table 1 in the appendix which inform on potential use of any competing method in an objective function for path generation.

Finalizing this discussion, special attention must be given to the work of *Khan et al.* where trained AI models are employed to return a possible four-bar mechanism for the given desired path. They apply the Broyden–Fletcher–Goldfarb–Shanno algorithm which is commonly available in MATLAB. Traditional optimization for path generating mechanisms can take anywhere from one to ten hours, and maybe AI can speed up this process. Their algorithm runs in $\sim \mathcal{O}(n^2)$ which is considerably slow (Brownlee (2021)). However if we compare it with traditional methods such as Genetic Algorithms ($\sim \mathcal{O}(n)$), Differential evolution ($\sim \mathcal{O}(n)$) or Non-Dominated Sorting ($\sim \mathcal{O}(n^2)$) it does not seem a prize winner. Though it is in the same range, and built using a simple toolbox in MATLAB, therefore indicating its potential, and one can only wonder what an optimized AI could provide for more complex mechanisms than four-bar linkages.

5. CONCLUSION

This review has illuminated the integration of metamaterials studied as elastic structures with both individual and collective dynamics. We have evaluated the advantages and disadvantages within the mixed grey zone, where both frozen and vibrating units coexist. Additionally, potential variable Poisson ratios, based on auxetic rotating squares, have been aligned with the blueprint of these collective metamaterials and dynamics, introducing a spin-off from existing quasi-static approaches. Alongside this, we have underscored the enhancements in power usage and curving closing resulting from the inclusion of dynamics. A critical perspective has been presented on existing path-generating mechanisms, whether rigid-link or compliant, and whether experimentally proven or not. We have compared various shape-distinguishing methods, discussed objective functions, and evaluated the promising path toward AI-driven mechanism design in contrast to traditional synthesis algorithms. It is essential to note that this literature review cannot encompass all relevant literature, and only a selective subset has been considered. Furthermore, the relatively novel field of mechanical metamaterials, while extensively researched, is still in its early stages, limiting immediate connections to practical applications. In summary, the individual realms of mechanical metamaterials and path generation have been thoroughly studied and established. However, it is crucial to emphasize that their combination has not been explored until the present day. The fusion of these fields appears highly beneficial across various sectors. Through this review, we provide a realistic answer to the research question, 'How can mechanical metamaterials generate closed end-effector paths with a single input?' This not only addresses the query but also unveils new avenues for further research.

REFERENCES

Arkin, E. M. (1989). An Efficiently Computable Metric for Comparing Polygonal Shapes. *IEEE Transactions on Pattern Analysis and Machine Intelligence*, *13*(3).

Avbelj, J., Muller, R., & Bamler, R. (2015). A metric for polygon comparison and building extraction evaluation. *IEEE Geoscience and Remote Sensing Letters*, *12*(1), 170–174. doi:

Baconnier, P., Shohat, D., López, C. H., Coulais, C., Démery, V., Düring, G., & Dauchot, O. (2022, 10). Selective and collective actuation in active solids. *Nature Physics*, *18*(10), 1234–1239.

Baisch, A. T. (2011). *HAMR3: An Autonomous 1.7g Ambulatory Robot*. IEEE.

Banerjee, A., Bhattacharya, B., & Mallik, A. K. (2009, 2). Forward and inverse analyses of smart compliant mechanisms for path generation. *Mechanism and Machine Theory*, *44*(2), 369–381.

Brownlee, J. (2021, 1). *A gentle introduction to the BFGS Optimization Algorithm.* Retrieved from `https://machinelearningmastery.com/bfgs-optimization-in-python/`

Bückmann, T., Thiel, M., Kadic, M., Schittny, R., & Wegener, M. (2014, 6). An elasto-mechanical unfeelability cloak made of pentamode metamaterials. *Nature Communications*, *5*.

Cabrera, J. A., Nadal, F., Muñoz, J. P., & Simon, A. (2007, 7). Multiobjective constrained optimal synthesis of planar mechanisms using a new evolutionary algorithm. *Mechanism and Machine Theory*, *42*(7), 791–806.

Cabrera, J. A., Ortiz, A., Nadal, F., & Castillo, J. J. (2011, 2). An evolutionary algorithm for path synthesis of mechanisms. *Mechanism and Machine Theory*, *46*(2), 127–141.

Cabrera, J. A., Simon, A., & Prado, M. (2002). Optimal synthesis of mechanisms with genetic algorithms. *Mechanism and Machine Theory*, *37*, 1165–1177. Retrieved from `www.elsevier.com/locate/mechmt`

Cheng, Y., Song, P., Lu, Y., Chew, W. J. J., & Liu, L. (2022). Exact 3D Path Generation via 3D Cam-Linkage Mechanisms. *ACM Transactions on Graphics*, *41*(6).

Cheng, Y., Sun, Y., Song, P., & Liu, L. (2021, 12). Spatial-temporal motion control via composite cam-follower mechanisms. *ACM Transactions on Graphics*, *40*(6), 1–15.

Chiandussi, G., Bugeda, G., & Oñate, E. (2000). Shape variable definition with C0, C1 and C2 continuity functions. *Computer methods in applied mechanics and engineering*, *188*, 727–742. Retrieved from `www.elsevier.com/locate/cma`

Cosgriff, R. (1960). Identification of shape. *Ohio State Univ. Res. Foundation, Columbus, Rep. 820-11*.

Coulais, C., Teomy, E., De Reus, K., Shokef, Y., & Van Hecke, M. (2016, 7). Combinatorial design of textured mechanical metamaterials. *Nature*, *535*(7613), 529–532.

Grima, J. N., & Caruana-Gauci, R. (2012). Mechanical metamaterials: Materials that push back. *Nature Materials*, *11*(7), 565–566.

Grima, J. N., & Evans, K. E. (2000). Auxetic behavior from rotating squares. *Journal of Materials Science Letters*, 1563–1565.

Guo, L., Zhang, Y., Wu, J., & Yao, Y. a. (2023, 9). Combination of different trajectory description approaches improves the trajectory synthesis performance: Validation by a coarse-to-fine method. *Mechanism and Machine Theory*, *187*. doi:

Kadic, M., Bückmann, T., Stenger, N., Thiel, M., & Wegener, M. (2012, 5). On the practicability of pentamode mechanical metamaterials. *Applied Physics Letters*, *100*(19).

Kempe, A. (1875). On a General Method of describing Plane Curves of the nth degree by Linkwork. *Proceedings of The London Mathematical Society*.

Khan, N., Ullah, I., & Al-Grafi, M. (2015, 4). Dimensional synthesis of mechanical linkages using artificial neural networks and Fourier descriptors. *Mechanical Sciences*, *6*(1), 29–34. doi:

Kota, S., Hetrick, J., Li, Z., & Saggere, L. (1999). Tailoring Unconventional Actuators Using Compliant Transmissions: Design Methods and Applications. *TRANSACTIONS ON MECHATRONICS*, *4*(4).

Lakes, R., Lee, T., & Bersie, A. (2001, 3). Extreme Damping in Composite Materials with Negative-stiffness Inclusions. *Nature*, *410*, 565–567.

Lee, D. J., Antani, S., & Long, L. R. (2003). Similarity Measurement Using Polygon Curve Representation and Fourier Descriptors for Shape-based Vertebral Image Retrieval. *Medical Imaging: Image Processing*, *5032*, 1283–1291. Retrieved from http://proceedings.spiedigitallibrary.org/

Lin, C., Nicaise, S. M., Lilley, D. E., Cortes, J., Jiao, P., Singh, J., … Bargatin, I. (2018, 12). Nanocardboard as a nanoscale analog of hollow sandwich plates. *Nature Communications*, *9*(1).

Mankame, N. D., & Ananthasuresh, G. K. (2007). Synthesis of contact-aided compliant mechanisms for non-smooth path generation. *International Journal for Numerical Methods in Engineering*, *69*(12).

Mendeley - Reference Management Software. (2024).

Nadal, F., Cabrera, J. A., Bataller, A., Castillo, J. J., & Ortiz, A. (2015, 6). Turning functions in optimal synthesis of mechanisms. *Journal of Mechanical Design*, *137*(6). doi:

News, R., & Lakes, R. (1993). Advances in Negative Poisson's Ratio Materials **. *Advanced Materials*, *5*(4), 293–296.

Nicolaou, Z. G., & Motter, A. E. (2012). Mechanical metamaterials with negative compressibility transitions. *Nature Materials*, *11*(7), 608–613.

Pathak, V. K., Singh, R., Sharma, A., Kumar, R., & Chakraborty, D. (2023, 3). A Historical Review on the Computational Techniques for Mechanism Synthesis: Developments Up to 2022. *Archives of Computational Methods in Engineering*, *30*(2), 1131–1156.

Rafsanjani, A., Bertoldi, K., & Studart, A. R. (2019). Programming soft robots with flexible mechanical metamaterials. *Science Robotics*, *4*(29).

Rai, A. K., Saxena, A., & Mankame, N. D. (2010, 6). Unified synthesis of compact planar path-generating linkages with rigid and deformable members. *Structural and Multidisciplinary Optimization*, *41*(6), 863–879.

Research Rabbit. (2024).

Russell, K., & Sodhi, R. S. (2001, 3). Kinematic synthesis of adjustable RRSS mechanisms for multi-phase motion generation. *Mechanism and Machine Theory*, *36*, 939–952. Retrieved from www.elsevier.com/locate/mechmt

Sardashti, A., Daniali, H. M., & Varedi-Koulaei, S. M. (2022, 2). Geometrical Similarity Error Function-Innovative Adaptive Algorithm methodology in path generation synthesis of the four-bar mechanism using metaheuristic algorithms. *Proceedings of the Institution of Mechanical Engineers, Part C: Journal of Mechanical Engineering Science*, *236*(3), 1550–1570.

Saxena, A. (2005). Synthesis of compliant mechanisms for path generation using genetic algorithm. *Journal of Mechanical Design*, *127*(4).

Saxena, A., & Ananthasuresh, G. K. (2001a). Topology optimization of compliant mechanisms with strength considerations. *Mechanics of Structures and Machines*, *29*(2), 199–221.

Saxena, A., & Ananthasuresh, G. K. (2001b, 3). Topology synthesis of compliant mechanisms for nonlinear force–deflection and curved path specifications. *Journal of Mechanical Design, Transactions of the ASME*, *123*(1), 33–42.

Shaikeea, A. J. D., Cui, H., O'Masta, M., Zheng, X. R., & Deshpande, V. S. (2022, 3). The toughness of mechanical metamaterials. *Nature Materials*, *21*(3), 297–304.

Shiakolas, P. S., Koladiya, D., & Kebrle, J. (2002, 12). On the optimum synthesis of four-bar linkages using differential evolution and the geometric centroid of precision positions. *Inverse Problems in Engineering*, *10*(6), 485–502.

Siéfert, E., Reyssat, E., Bico, J., & Roman, B. (2019, 1). *Bio-inspired pneumatic shape-morphing elastomers* (Vol. 18) (No. 1). Nature Publishing Group.

Sigmund, O. (1997). On the Design of Compliant Mechanisms Using Topology Optimization*. *Mechanical Structures & Machines*, *25*(4), 493–524.

Storn, R., & Price, K. (1997). Differential Evolution-A Simple and Efficient Heuristic for Global Optimization over Continuous Spaces. *Journal of Global Optimization*, *11*, 341–359.

Surjadi, J. U., Gao, L., Du, H., Li, X., Xiong, X., Fang, N. X., & Lu, Y. (2019, 3). *Mechanical Metamaterials and Their Engineering Applications* (Vol. 21) (No. 3). Wiley-VCH Verlag.

Swan, C. C., & Rahmatalla, S. F. (2004, 9). *DESIGN AND CONTROL OF PATH-FOLLOWING COMPLIANT MECHANISMS* (Tech. Rep.). Salt Lake City, Utah USA: Computers and Information in Engineering Conference.

Tantanawat, T., & Kota, S. (2006). DESIGN OF COMPLIANT MECHANISMS FOR MINIMIZING INPUT POWER IN DYNAMIC APPLICATIONS. In *Asme international design engineering technical conferences & computers and information in engineering conference*. Philadelphia. Retrieved from http://www.asme.org/about-asme/terms-of-use

Torres-Moreno, J. L., Cruz, N. C., Álvarez, J. D., Redondo, J. L., & Giménez-Fernandez, A. (2022, 3). An open-source tool for path synthesis of four-bar mechanisms. *Mechanism and Machine Theory*, *169*. doi:

Ullah, I., & Kota, S. (1997). *Optimal Synthesis of Mechanisms for Path Generation Using Fourier Descriptors and Global Search Methods* (Tech. Rep.). Retrieved from http://www.asme.org/about-asme/terms-of-use

Volotão, C. F. S., Santos, R. D. C., Erthal, G. J., & Dutra, L. V. (2010). Shape characterization with turning functions. In *International conference on systems, signals and image processing* (Vol. 17).

W Pedersen, C. B., Buhl, T., & Sigmund, O. (2001). Topology synthesis of large-displacement compliant mechanisms. *INTERNATIONAL JOURNAL FOR NUMERICAL METHODS IN ENGINEERING Int. J. Numer. Meth. Engng*, *50*, 2683–2705.

Zadpoor, A. A. (2016, 9). *Mechanical meta-materials* (Vol. 3) (No. 5).

Royal Society of Chemistry.
Zahn, C. T., & Roskies, R. Z. (1972). Fourier Descriptors for Plane Closed Curves. *IEEE TRANSACTIONS ON COMPUTERS*, *C-21*(3).
Zhang, D., & Lu, G. (2004). Review of shape representation and description techniques. *Pattern Recognition*, *37*(1), 1–19. doi:

APPENDIX

Method/Property	Application	Computation	Invariance	Downsides	Proof of concept
Brute force	Very easy	Hard ($\mathcal{O}(n^2)$)	None	Many calculations	PG performed in 4BL
Turning function	Easy/Moderate	Moderate ($\mathcal{O}(n)$)	Angle | Position	Other shape, same area	PG performed in 4BL
NSDVs	Moderate	Moderate ($\mathcal{O}(n)$)	None	Simple polygons only	PG performed in 4BL
Fourier descriptors	Moderate	Moderate ($\mathcal{O}(n)$)	Size | Angle | Position	Path might not close	PG performed in 4BL
PoLiS	Easy	Moderate ($\mathcal{O}(n)$)	None	No path generation yet	2D building recognition

Table 1. Comparison between shape features and their application in optimization, PG = Path generation, 4BL = Four-bar linkage

3 Supplementary Information

This section provides all the details regarding the modeling, the actuator, the manufacturing, the assembly, and the experiments conducted in the thesis, as referenced in the main text.

Supplementary Materials

Supplementary information to the main paper: 'Dynamical Metamaterials for Path Generation'

Tom Vreugdenhil

Vreugdenhil

This PDF file includes:

Figs. S1 to S20
Tables S1 to S2

1. Xeryon XLA-5-55-1250 Actuator Specifications

The actuator used in the robotic prototype is a miniature linear piezo stepper made by Xeryon in Belgium. In this instance the specific XLA-5-55-1250 where 5 denotes the holding and driving force, 55 denotes the total travel in millimeters and 1250 the encoder precision in nanometers. It can operate at speeds ranging from from 5 μm/s to 400 mm/s, and accelerate with 840 m/s^2. It comes with a controller board, which can be connected to a computer with or without Arduino.

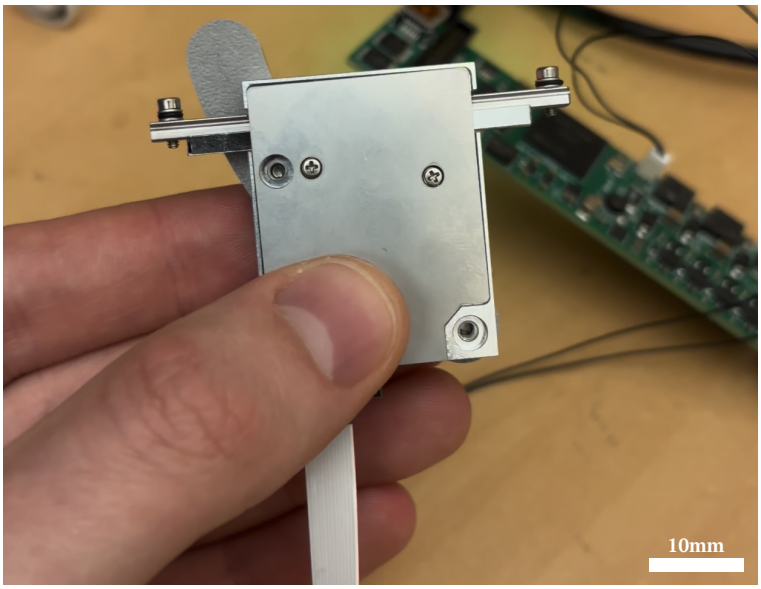

Fig. 1. XLA-5-55-1250 actuator, with controller in background

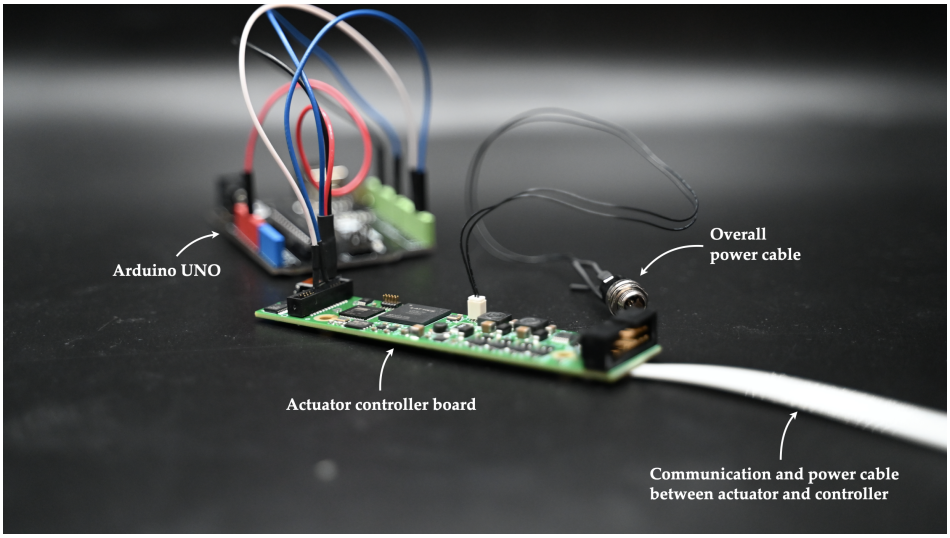

Fig. 2. Controller board, powercables and Arduino UNO in the background

2. Assembly steps

After 3D printing two identical metamaterial specimens, some mounting brackets and spacers for the actuator, and the actuator itself, assembly is done in few easy steps which only require a vise, two steel pins ($\phi 1.6x20mm$) for the rotation joints at the top and one steel pin ($\phi 2x50mm$) for the rotation joints at the bottom. In the figures below, the $\phi 1.6x20mm$ pins are already press-fit into the actuator bracket. The vice is required to press-fit the $\phi 2x50mm$ pin into one metamaterial, then every component is simply stacked on top of each other, and at last the second metamaterial is press-fit onto the remainder of the $\phi 2x50mm$ steel pin completing the assembly. The actuator is now effectively sandwiched in between two metamaterials. The only final touch is placing rubber stops on the end of the $\phi 1.6x20mm$ pins to make sure the top actuated block does not slide off during operation (safety precaution).

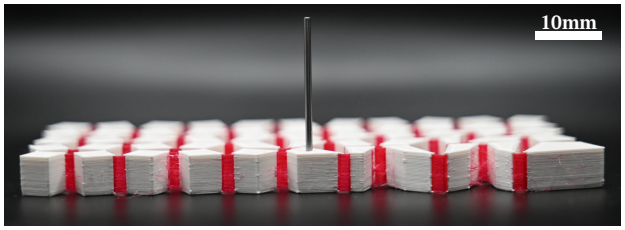

(a) Single metamaterial 3D print, with press-fitted steel pin ($\phi 2x50mm$) into the lower actuated block

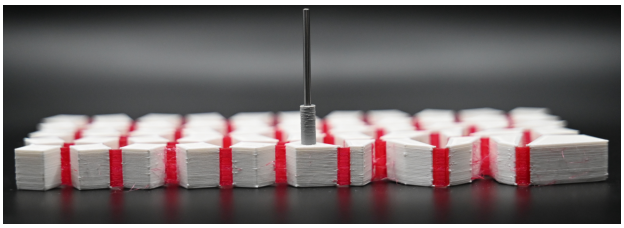

(b) Single metamaterial 3D print, with press-fitted steel pin ($\phi 2x50mm$) into the lower actuated block, and one spacer

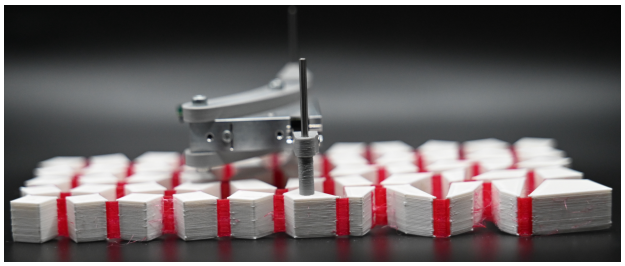

(c) Single metamaterial 3D print, with press-fitted steel pin ($\phi 2x50mm$) into the lower actuated block, one spacer, and the actuator slid over the pin. The pin already press-fit into the actuator bracket loosely slides into the top actuated block.

(d) Single metamaterial 3D print, with press-fitted steel pin ($\phi 2x50mm$) into the lower actuated block, one spacer, the actuator slid over the pin, and the second spacer.

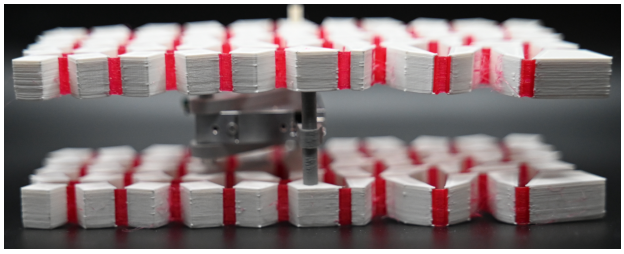

(e) Single metamaterial 3D print, with press-fitted steel pin ($\phi 2x50mm$) into the lower actuated block, one spacer, the actuator slid over the pin, the second spacer, and the second metamaterial 3D print press-fit onto the steel pin ($\phi 2x50mm$).

Fig. 3. Assembly steps for the single metamaterial 3D print with steel pin and spacers.

3. Finished robotic metamaterial prototype

(a) Front view of the robotic prototype, showing the actuator sandwiched between the metamaterials.

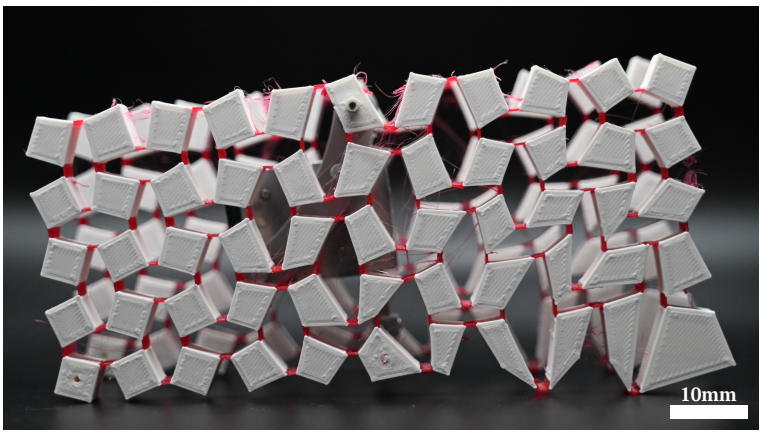

(b) Side view of the robotic prototype.

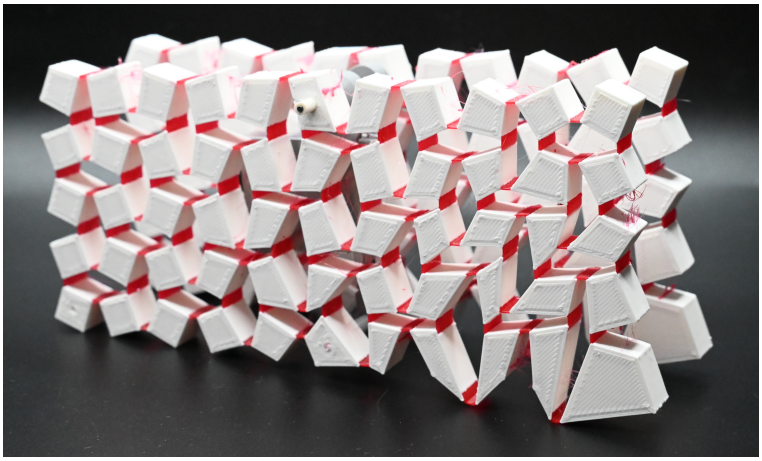

(c) Perspective view of the robotic prototype.

Fig. 4. Three views of the robotic metamaterial prototype: front, side, and perspective.

4. Model stiffness and damping tuning

The model contains three parameters for stiffness: $k_{stretch}$, k_{shear}, k_{rot} (see Figure 2). Damping values are a function of the stiffnesses, with a scaling factor to distinguish between x/y and rotation. Characterizing the stiffness of the 3D printed TPU hinges meant fabricating a structure with a known total stiffness as a function of $k_{stretch}$, k_{shear} and k_{rot}. This structure is a four by four set of rigid PLA blocks with TPU hinges in between. This structure is clamped in vices in a Instron 5900 series with a 50N load cell, and a tensile/compression test is performed in tensile and shear direction of the test specimen by deforming the specimen with positive and negative displacement to account for tension and compression. This data is fitted with the stiffness model for the test specimen (Figure 7) and by optimizing the model parameters a good fit is found for stiffness values $k_{stretch}$, k_{shear} and k_{rot} to align with the measured Instron data.

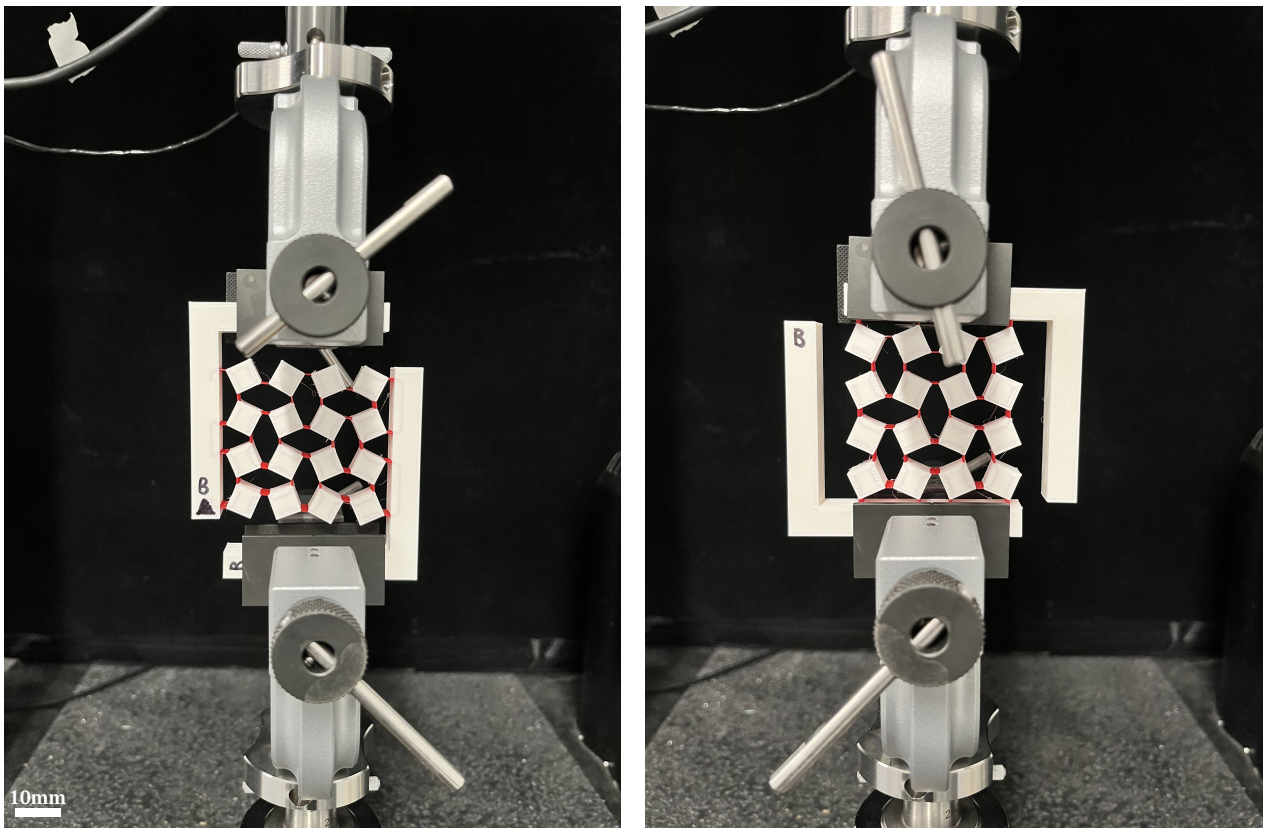

(a) Shearing measurement on PLA/TPU testspecimen B

(b) Stretching measurement on PLA/TPU testspecimen B

Fig. 5. Instron shearing and stretching measurement on a 4x4 blocky metamaterial

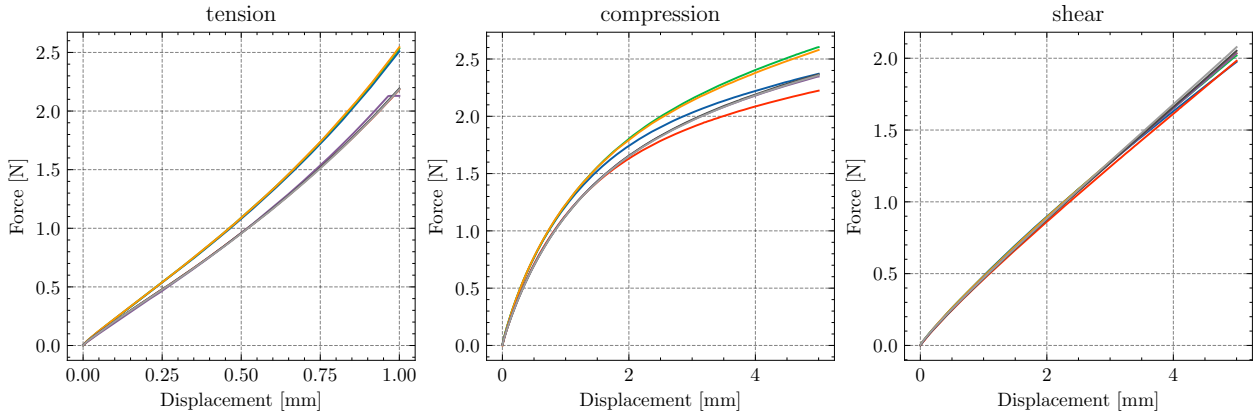

Fig. 6. Stiffness graphs for all measurements, on specimen A and B, in tension, compression and shear. Every specimen was measured with three runs, where each run consists of four loading cycles.

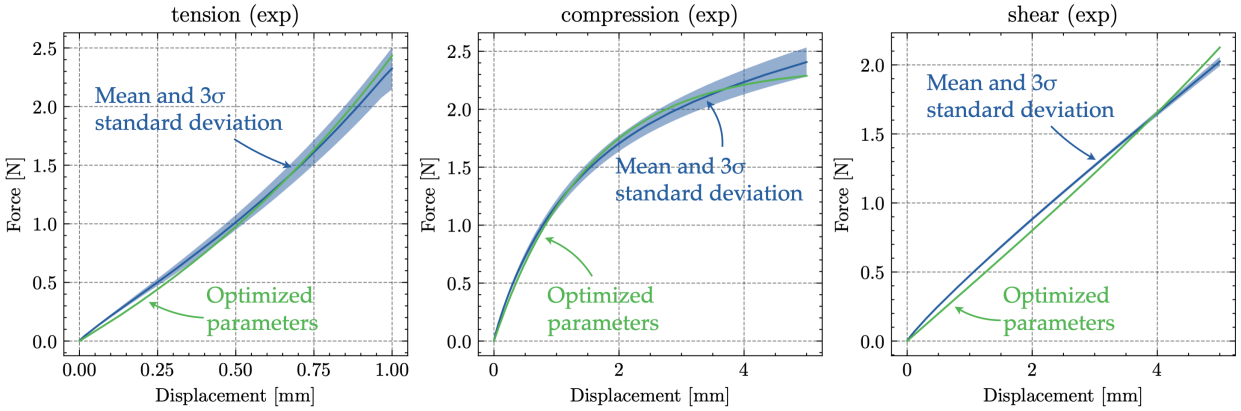

Fig. 7. Stiffness graphs where the measurement data is bundled into a mean with standard deviation and the result of optimizing the model to fit this measurement data

Method	Stretch ($k_{stretch}$) [N/mm]	Shear (k_{shear}) [N/mm]	Rotation (k_{rot}) [N/mm]
Static	19.48	1.417	0.1760

Table 1. Optimized stiffness model to match the instron measurement data

Static testing of the hinges is now complete, but during dynamic experiments it was found that the TPU hinges do not comply with just static stiffness, and more testing was required to unravel dynamic stiffnesses. By actuating a optimized metamaterial and tracking the endeffector displacement there was new, dynamical, measurement data. This time parameter tuning had to be done manually, and through endless variations of stiffness and damping parameters new values were found to achieve a good fit.

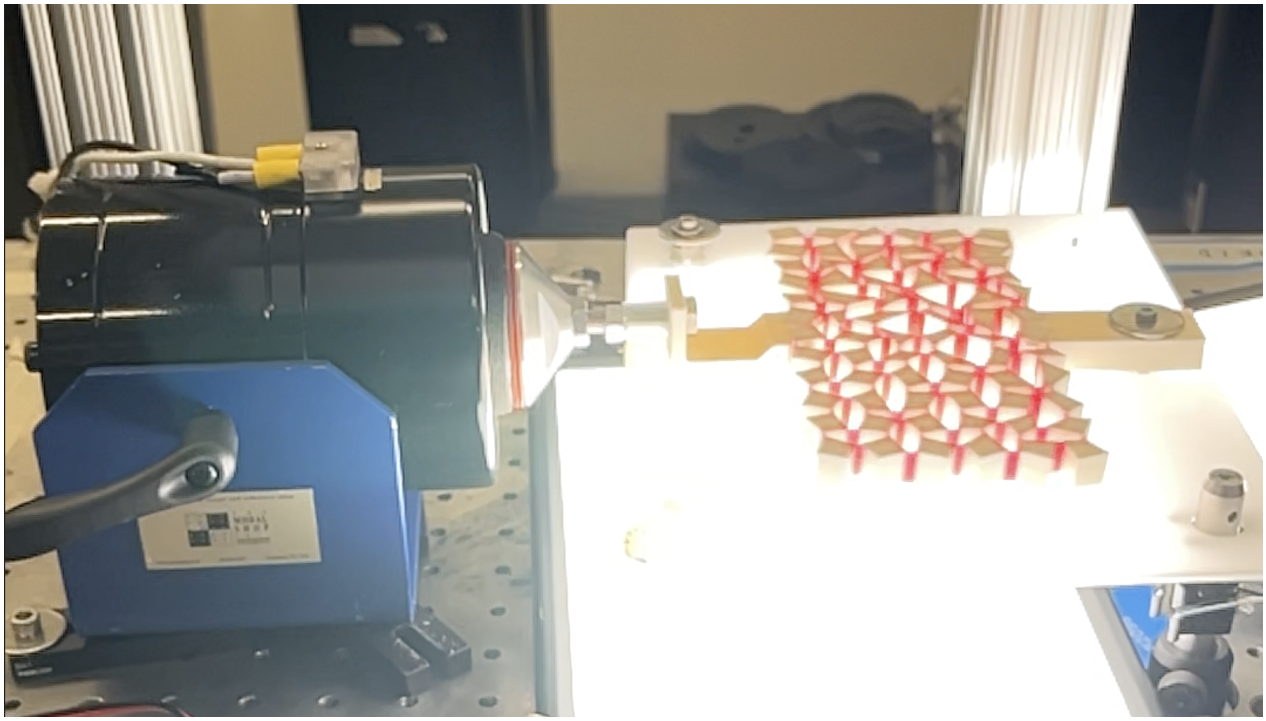

Fig. 8. Dynamic testing with a shaker, metamaterial design, appropriate constraints, light panel, and a high-speed camera on top (not visible)

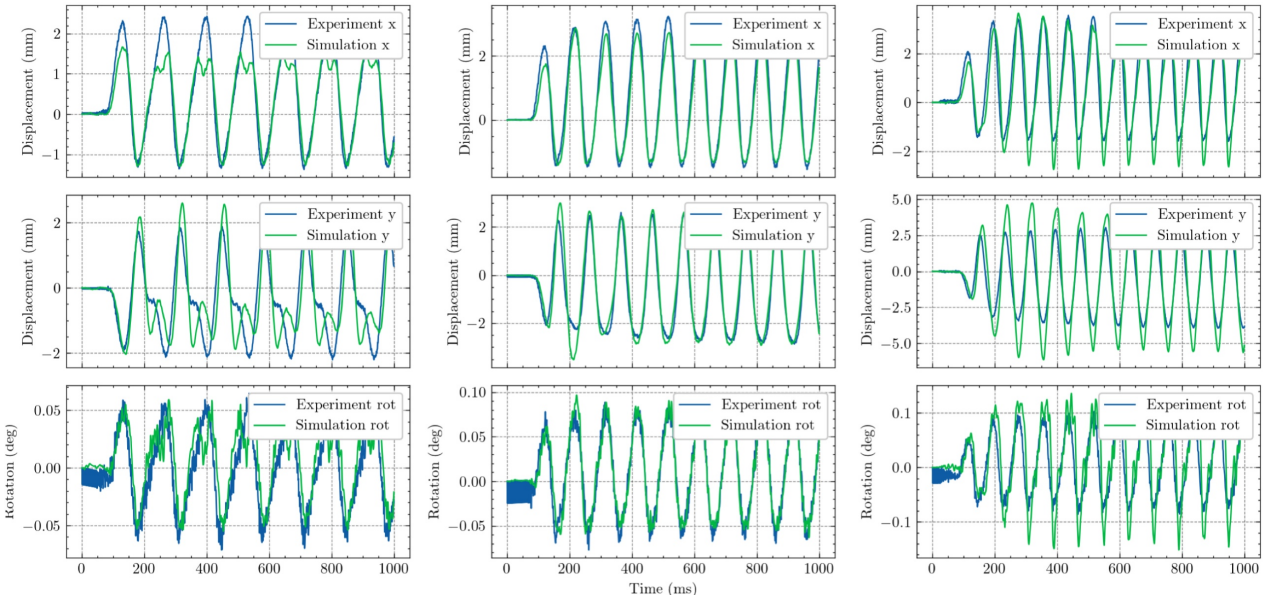

Fig. 9. Horizontal, vertical, and rotation deformation for a certain block on the metamaterial, actuated at 15, 20 and 25 [Hz]. By varying the stiffness parameters, the best alignment of experiment and simulation had to be found.

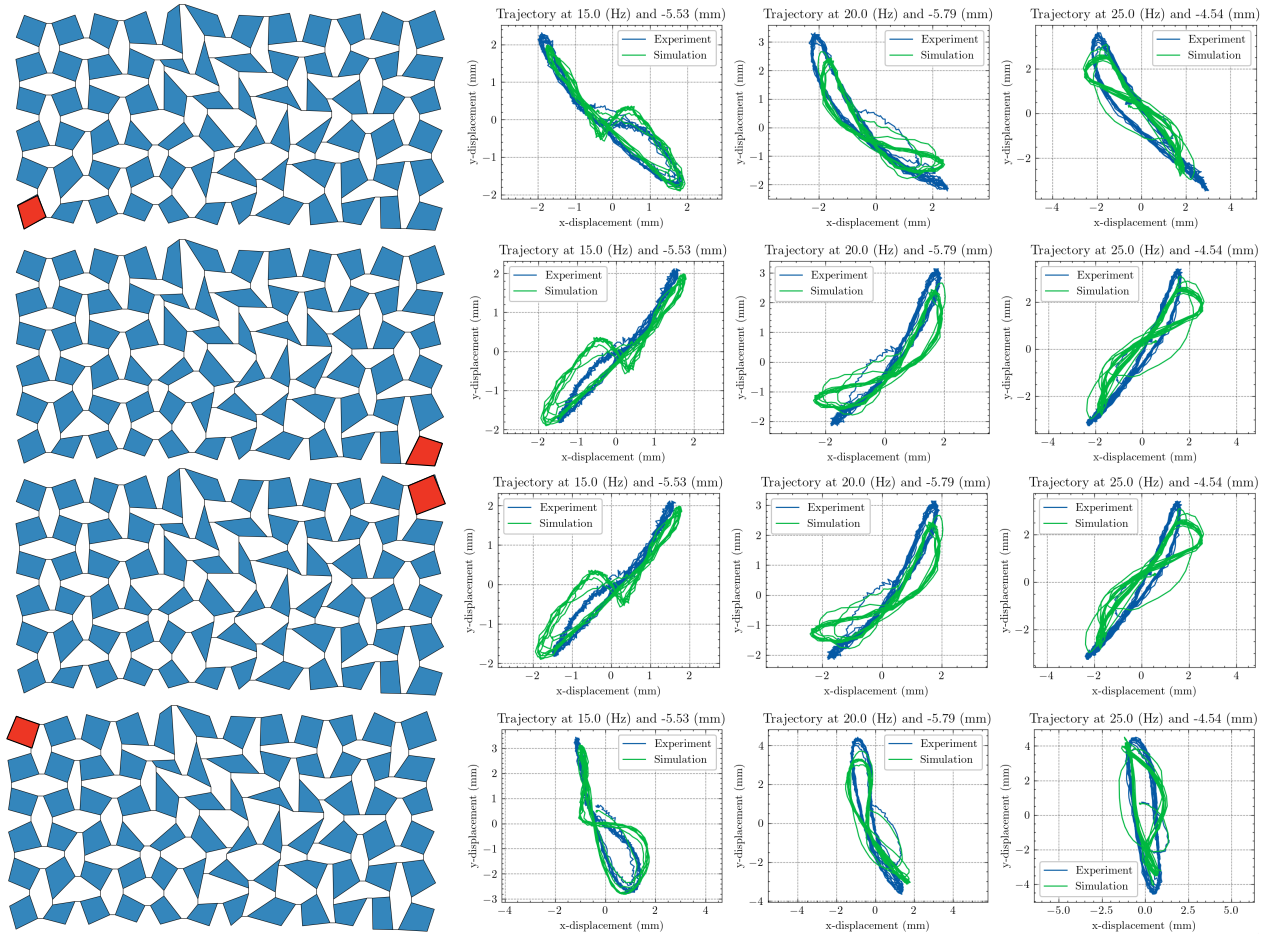

Fig. 10. Verification of the best stiffness parameters by overlaying the model and experiment trajectories for a selection of endeffector blocks (in red) within the metamaterial.

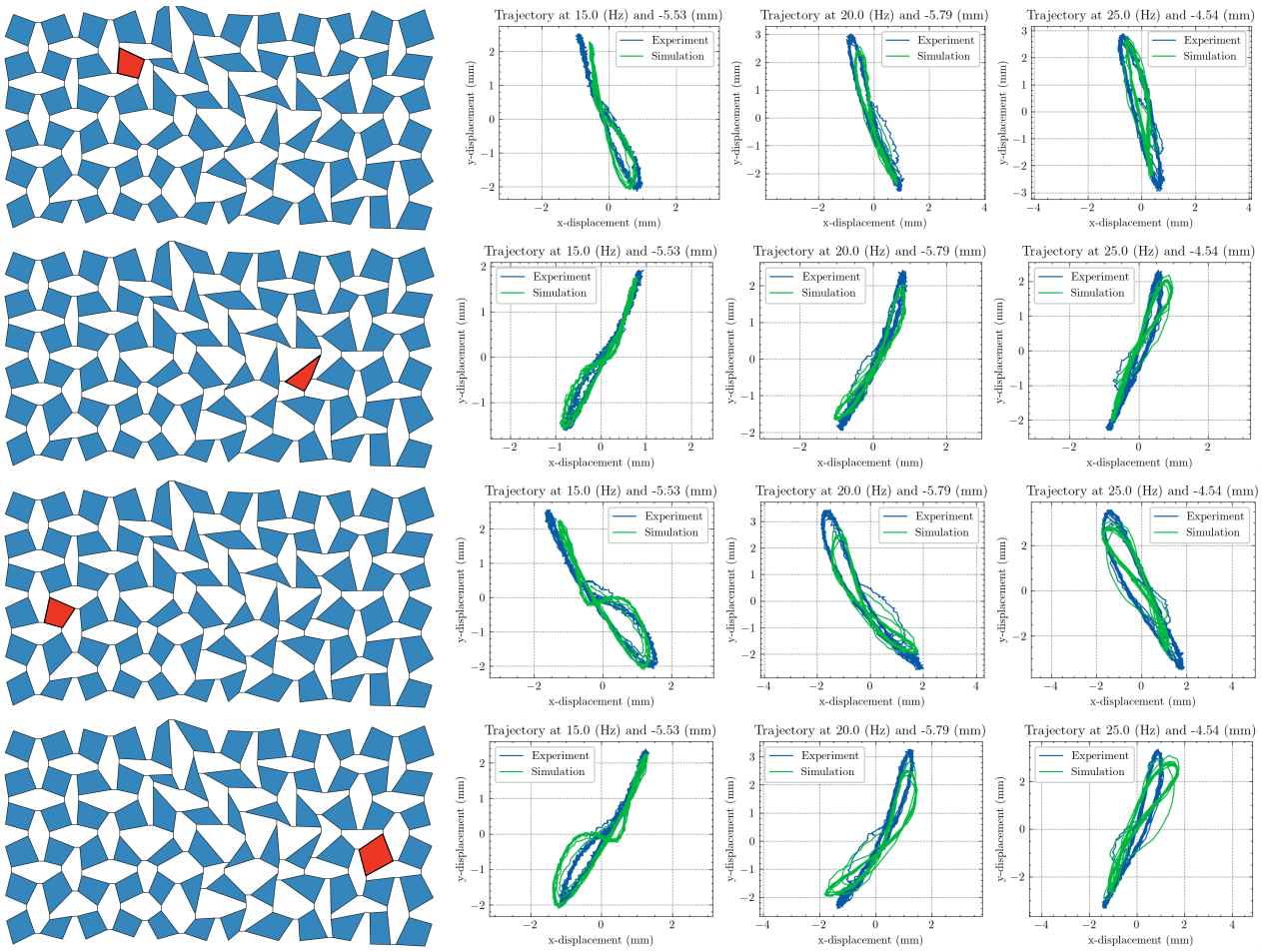

Fig. 11. Verification of the best stiffness parameters by overlaying the model and experiment trajectories for a selection of endeffector blocks (in red) within the metamaterial.

Method	Stretch ($k_{stretch}$) [N/mm]	Shear (k_{shear}) [N/mm]	Rotation (k_{rot}) [N/mm]
Static	19.48	1.417	0.1760
Dynamic	19.48	3.683	2.640

Table 2. Optimized stiffness models to match the Instron measurement data and the new dynamically tuned stiffness

Table 4 shows dynamic shear stiffness values of 2.6x the static value, and even 15x the static rotation stiffness in order to have a good alignment. This can hint toward stiffness models that contain higher-order stiffness terms. The stiffness values that align with the deformation in Figure 12 below are not known exactly.

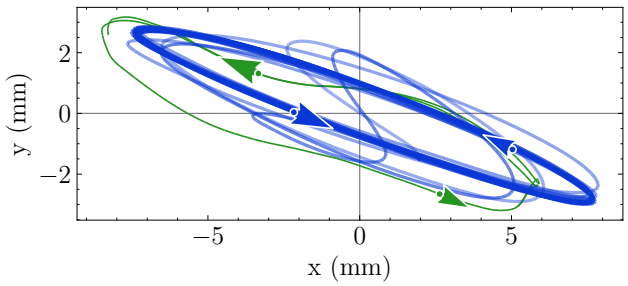

Fig. 12. 50% scaled-down simulation results in green, and experiment in blue.

5. Manufacturing

The manufacturing process for these PLA and TPU 3D printed metamaterials is streamlined and results in high quality prototypes. The figures below highlight some more details in the process.

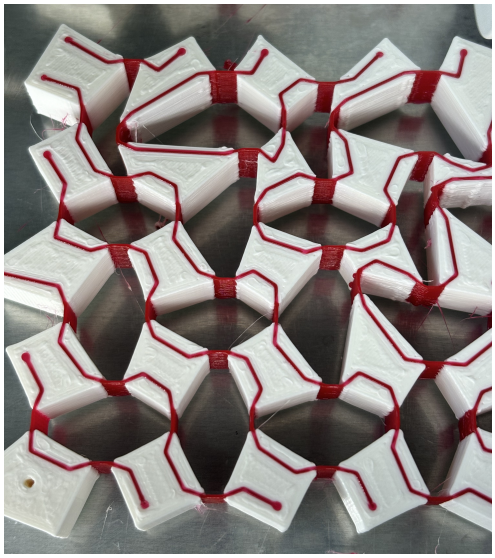

(a) Closeup of PLA and TPU 3D printing, clearly visible is the fully fixed red TPU material in the white PLA blocks.

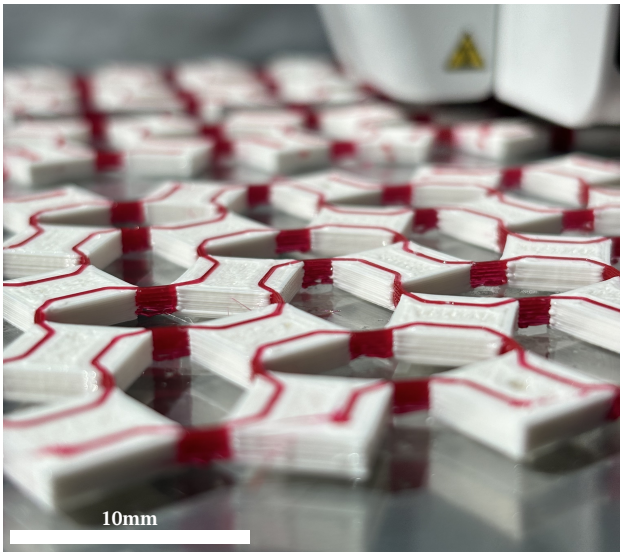

(b) Closeup of PLA and TPU 3D printing, clearly visible is the fully fixed red TPU material in the white PLA blocks.

Fig. 13. Detailed pictures of the 3D printing process with two materials.

Fig. 14. Perspective view on the PLA and TPU 3D printing process.

6. Experiment figures

The experimental setup for the robotic metamaterial consisted of a black floor and backdrop for the walking experiment and a vise in front of a black backdrop for the clamped experiment. For both scenarios, below are additional pictures explaining the situation.

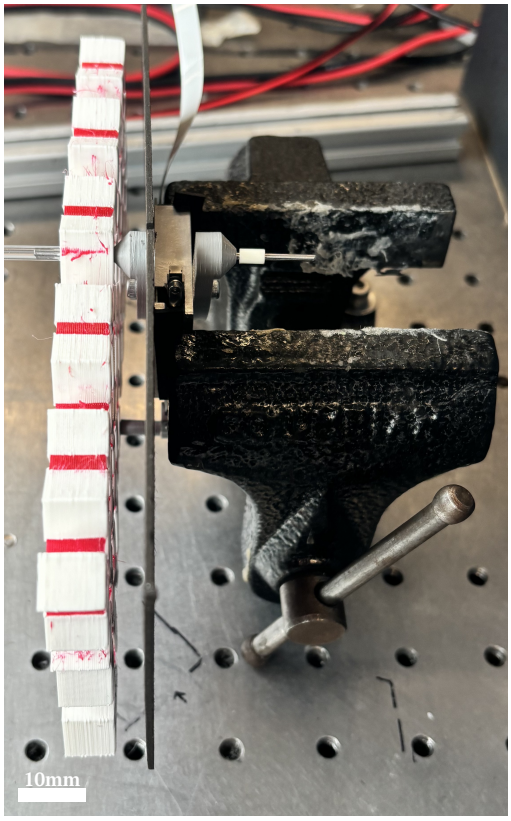

(a) Side view of the clamped experiment, where the actuator body is clamped in a vise, thereby fixing one of the actuator blocks.

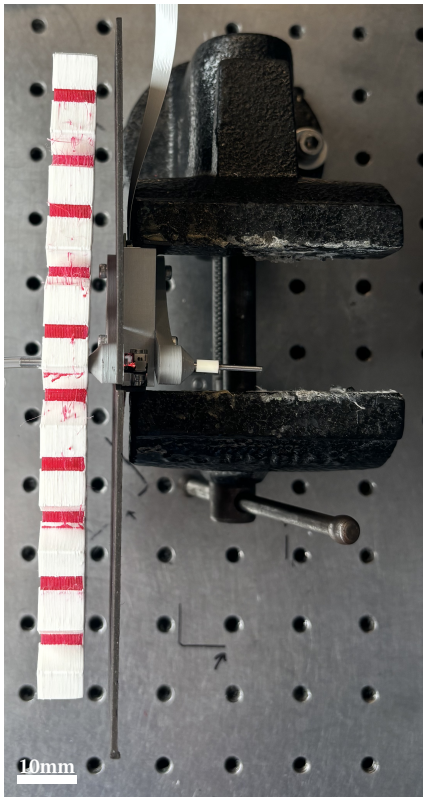

(b) Top view of the clamped experiment, where the actuator body is clamped in a vise, thereby fixing one of the actuator blocks. The black cardboard sheet is there to create a better contrast when recording.

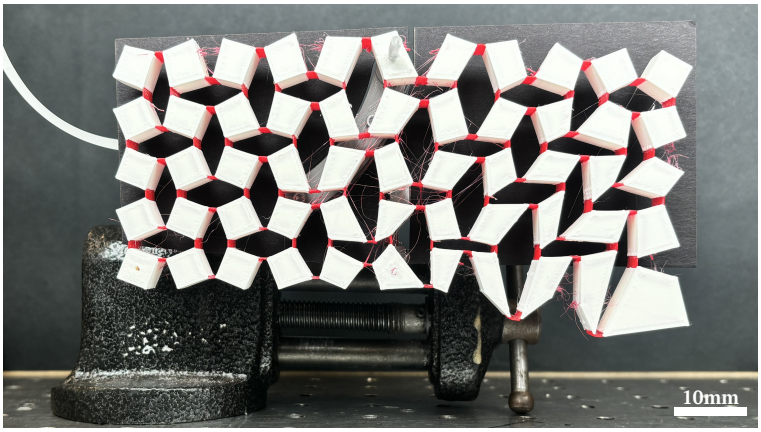

(c) Front view of the clamped experiment, where the actuator body is clamped in a vise, thereby fixing one of the actuator blocks. The black cardboard sheet is there to create a better contrast when recording.

Fig. 15. Three views of the clamped experiment in the vise

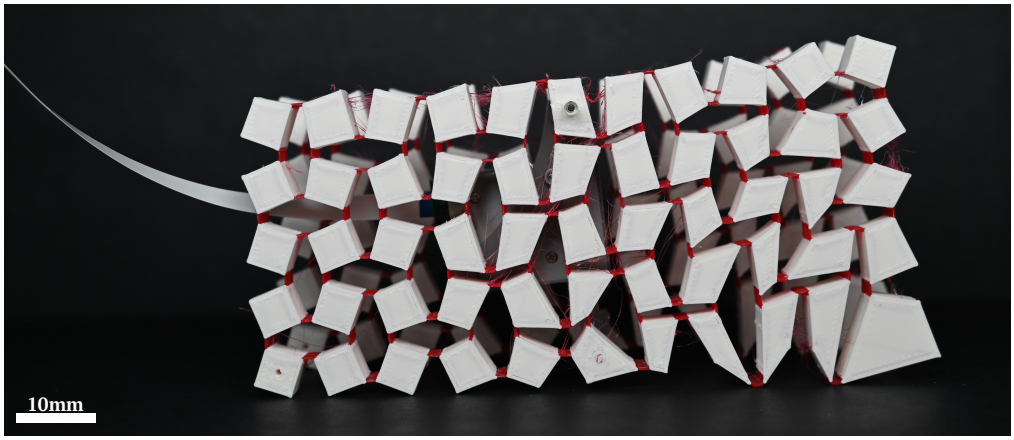

(a) Side view of the robotic metamaterial in contact with the floor

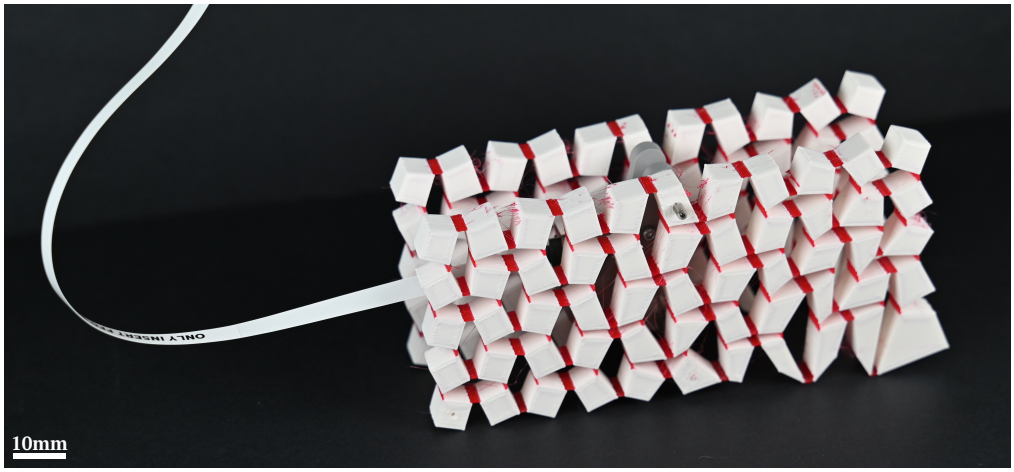

(b) Perspective view of the robotic metamaterial in contact with the floor

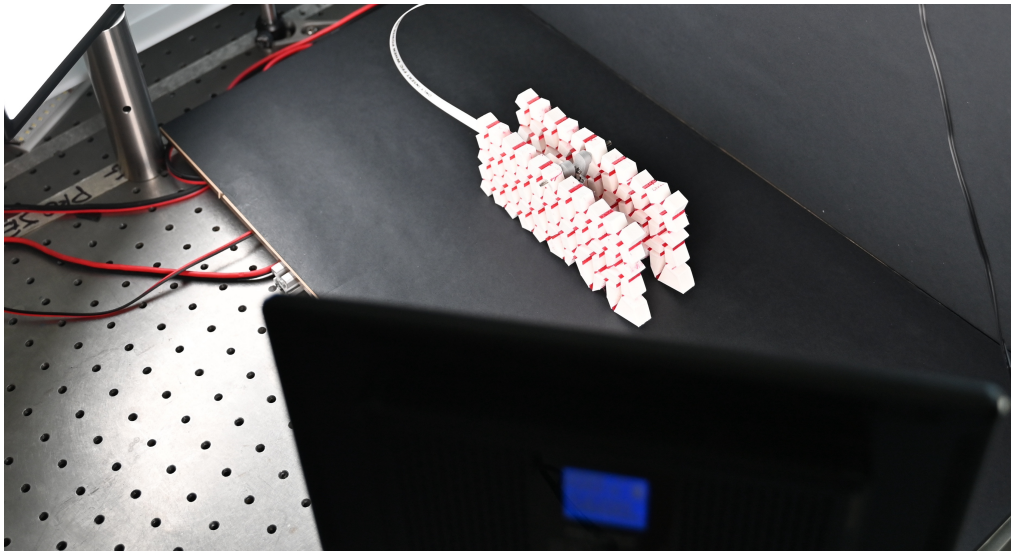

(c) Overview of the experiment environment with the black floor and backdrop, the lights and the robotic metamaterial

Fig. 16. Additional explanatory pictures of the conducted experiment with the robotic metamaterial in contact with the floor

7. Multi-gait experiment results

The results for multi-gait metamaterials with this design framework result in a simulation that can dynamically reprogram the directionality of endeffector trajectories. Experimentally, this directionality change was difficult to obtain.

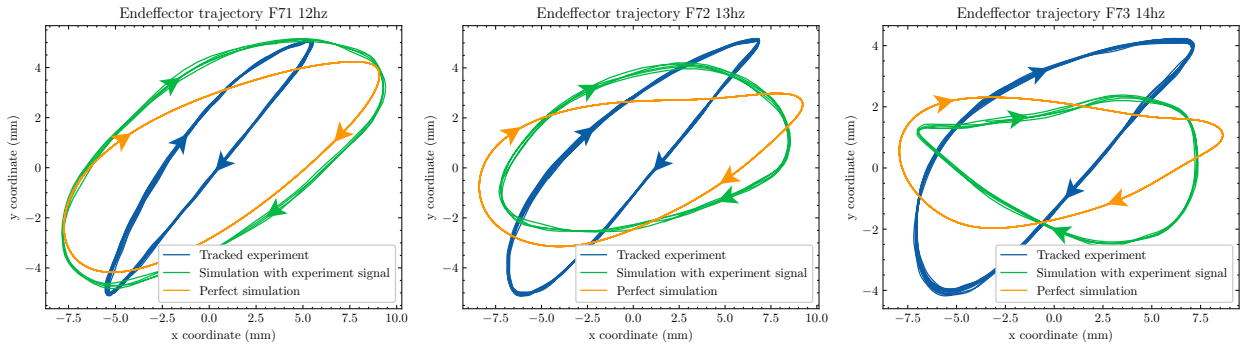

Fig. 17. Trajectories at 12, 13 and 14 [Hz]

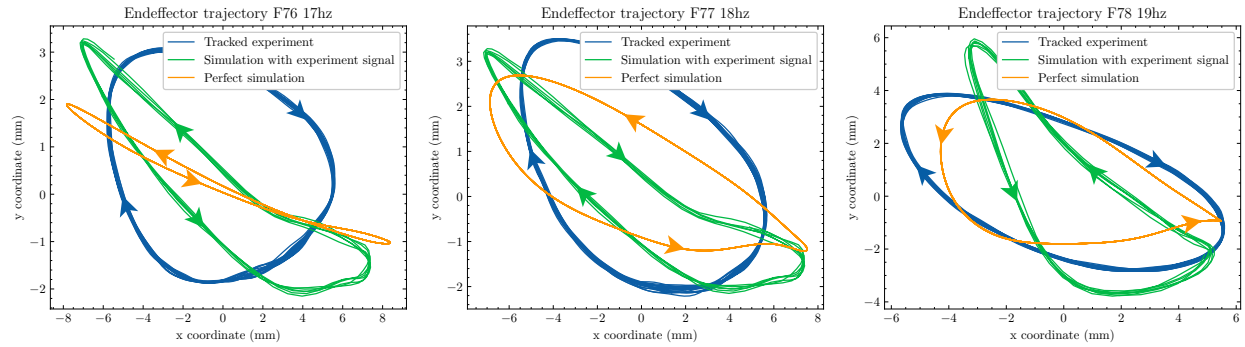

Fig. 18. Trajectories at 17, 18 and 19 [Hz]. The blue trajectory indicates the experiment where the endeffector has been tracked, the green line indicates simulation results where the actuation signal comes from tracking the experiment input, and the yellow line indicates the simulation with a perfect sinusoidal input signal.

Clearly, the perfect simulation in yellow does change direction at 18Hz, but the experiment does not. Even the simulation where the actuation signal is replaced by the tracked actuation signal from the experiment (green) has a hard time switching direction at 18Hz and only does so at 19Hz.

8. Outlook multi-gait robotic metamaterial

Multi-gait robotic metamaterials are envisioned to have tremendous potential. With a single actuator, and by only varying the actuation parameters, or external influences, different endeffector trajectories can be made. Below, there are two scenarios where external environmental influences trigger a change in internal dynamics and reprogram the endeffector trajectory with different functionalities as a result. This results in the most autonomous version of a robotic metamaterial.

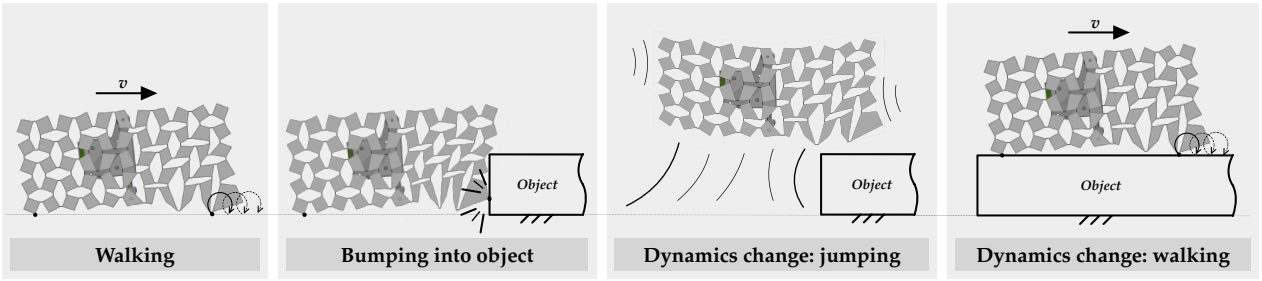

Fig. 19. Sideview of a robotic metamaterial, where bumping into an object triggers a change in dynamics where the metamaterial would jump over the obstacle. Afterwards the compression is no longer there, and the metamaterial returns to the normal internal dynamics.

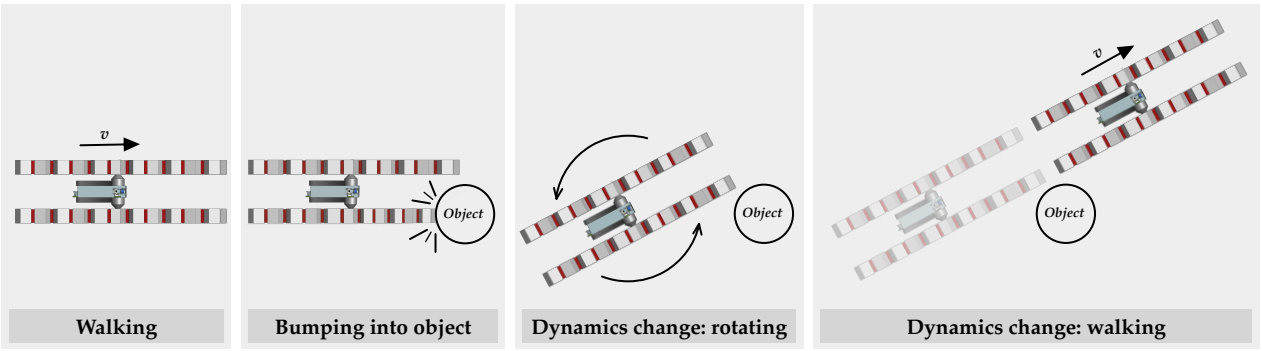

Fig. 20. Topview of a robotic metamaterial, where bumping into an object triggers a change in dynamics where the metamaterial would rotate to overcome the object in its way. Afterwards, the object is no longer there, and the metamaterial returns to the normal internal dynamics.